Table 1. Comparison of Clinical Factors Between Patients With and Without NR

Clinical category	SVR+TR	NR	Univariate *P* value	Multivariate odds (95% CI)	Multivariate *P* value
Patients, n	125	43		—	
Age and sex					
Age, y	57 (30–72)	56 (30–73)	.927	—	
Sex, male vs female	68 vs 57	24 vs 19	.872	—	
Liver histology					
F stage (F1–2 vs F3–4)	95 vs 30	20 vs 23	.001	6.35 (2.02–23.7)	.001
A grade (A0–1 vs A2–3)	68 vs 57	19 vs 24	.248	—	
Host gene factors					
IL-28B (TT vs TG/GG)[a]	109 vs 12	12 vs 31	<.001	19.7 (5.74–82.7)	<.001
ISGs (Mx, IFI44, IFIT1), (<3.5 vs ≥3.5)	103 vs 22	12 vs 31	<.001	5.26 (1.65–17.6)	.005
Metabolic factors					
BMI, kg/m^2	23.2 (16.3–34.7)	23.4 (19.5–40.6)	.439	—	
TG, mg/dL	98 (30–323)	116 (45–276)	.058	—	
T-Chol, mg/dL	167 (90–237)	160 (81–214)	.680	—	
LDL-Chol, mg/dL	82 (36–134)	73 (29–123)	.019	—	
HDL-Chol, mg/dL	42 (20–71)	47 (18–82)	.098	—	
FBS, mg/dL	94 (60–291)	96 (67–196)	.139	—	
Insulin, μU/mL	6.6 (0.7–23.7)	6.8 (2–23.7)	.039	—	
HOMA-IR	1.2 (0.3–11.7)	1.2 (0.4–7.2)	.697	—	
Fischer ratio	2.3 (1.5–3.3)	2.1 (1.5–2.8)	.005	8.91 (1.62–55.6)	.011
Other laboratory parameters					
AST level, IU/L	46 (18–258)	64 (21–283)	.017	—	
ALT level, IU/L	60 (16–376)	82 (18–345)	.052	—	
γ-GTP level, IU/L	36 (4–367)	75 (26–392)	<.001	—	
WBC, /mm^3	4800 (2100–11100)	4800 (2500–8200)	.551	—	
Hb level, g/dL	14 (9.3–16.6)	14.4 (11.2–17.2)	.099	—	
PLT, ×104/mm^3	15.7 (7–39.4)	15.2 (7.6–27.8)	.378	—	
Viral factors					
ISDR mutations ≤1 vs ≥2	80 vs 44	34 vs 9	.070	4.12 (1.25–15.9)	.019
HCV-RNA, KIU/mL	2300 (126–5000)	1930 (140–5000)	.725	—	
Treatment factors					
Total dose administered					
Peg-IFN, μg	3840 (960–7200)	3840 (1920–2880)	.916	—	
RBV, g	202 (134–336)	202 (36–336)	.531	—	
Achieved administration rate					
Peg-IFN, %					
≥80%	84	28	.975	—	
<80%	42	14			
RBV (%)					
≥80%	76	24	.745	—	
<80%	50	18			
Achievement of EVR	101/125 (81%)	0/43 (0%)	<.001	—	

BMI, body mass index; CI, confidence interval; FBS, fasting blood sugar; γ-GTP, gamma-glutamyl transpeptidase; Hb, hemoglobin; HDL-chol, high density lipoprotein cholesterol; LDL-chol, low density lipoprotein cholesterol; PLT, platelets; T-chol, total cholesterol; TG, triglycerides; WBC, leukocytes.

[a]IL-28B SNP at rs8099917.

instructions. The primer sequence for real-time detection PCR is given in the Supplementary Materials and Methods section. HCV RNA was detected as described previously[12] and expression was standardized to that of glyceraldehyde-3-phosphate dehydrogenase.

Reporter Assay

Construction of the interferon stimulated response element (ISRE)-luc reporter plasmid and Socs3-luc or Socs3 (FoxO binding element mutant [FBEmut])-luc reporter plasmids is described in the Supplementary Materials and Methods section.

Huh-7 cells were transfected with the ISRE-luc reporter plasmid 24 hours before IFN-alfa treatment. Cells were treated with IFN-alfa (0 or 100 U/mL) and BCAA (2 mmol/L) in low-amino-acid media. After 24 hours, luciferase activities were measured using the Dual Luciferase assay system (Promega, Madison, WI). For Socs3 promoter activities, Huh-7 cells were transfected with Socs3-luc or Socs3 (FBEmut)-luc reporter plasmids together with the Foxo3a expression plasmid, and luciferase activities were measured after 24 hours. Values were normalized to the luciferase activity of the co-transfected pGL4.75 Renilla luciferase-expressing plasmid (Promega).

Knockdown Experiments

Huh-7 cells were transfected with Ctrl (Stealth RNAi Negative Control Low GC Duplex #2; Invitrogen) or

targets (regulatory associated protein of mTOR [Raptor] and Foxo3a) (Supplementary Materials and Methods) small interfering RNA (siRNA) using Lipofectamine RNAiMAX reagent (Invitrogen) according to the manufacturer's instructions. After 48 hours, cells were cultured in normal or low-amino-acid media for a further 24 hours. The knockdown effect was confirmed by Western blotting.

Chromatin Immunoprecipitation Assay

Detailed experimental procedures are described in the Supplementary Materials and Methods section.

HCV Replication Analysis

pH77S3 is an improved version of pH77S, a plasmid containing the full-length sequence of the genotype 1a H77 strain of HCV with 5 cell culture-adaptive mutations that promote its replication in Huh-7 hepatoma cells.[13] pH77S.3/Gaussia luciferase (GLuc)2A is a related construct in which the GLuc sequence, fused to the 2A autocatalytic protease of foot-and-mouth virus RNA, was inserted in-frame between p7 and NS2[14] (Supplementary Materials and Methods). A signal sequence in GLuc directs its secretion into cell culture media, allowing real-time, dynamic measurements of GLuc expression to be performed without the need for cell lysis.

A 10-μg aliquot of synthetic RNA transcribed from pH77S.3/GLuc2A was used for electroporation. Cells were pulsed at 260 V and 950 μF using the Gene Pulser II apparatus (Bio-Rad Laboratories, Hercules, CA) and plated in fresh normal medium for 12 hours to recover. Cell medium was changed to ×1 DMEM without serum for 8 hours, then changed to low-amino-acid medium containing 0–8 mmol/L BCAA for a further 24 hours. Cells and culture medium were collected and used for GLuc assays, real-time detection PCR, and Western blotting. The number of viable cells was determined by a (3-[4,5-dimethylthiazol-2-yl]-5-[3-carboxymethoxyphenyl]-2-[4-sulfophenyl] -2H-tetrazolium, inner salt) assay (Promega).

Continuously JFH-1–infecting Huh-7 cells were obtained by the infection of Huh-7 cells with JFH-1 cell culture-derived HCV at a multiplicity of infection of 0.01. Cells were maintained in normal medium by passaging every 3–4 days for approximately 6 months. About 20%–30% of the cells consistently were positive for HCV core protein (Supplementary Figure 4). Culture medium of JFH-1–infecting Huh-7 cells was changed to the low-amino-acid medium containing 0–8 mmol/L BCAA for 24 hours. Cells then were collected and used for assays.

Statistical Analysis

Results are expressed as mean ± standard deviation. Significance was tested by 1-way analysis of variance with the Bonferroni method, and differences were considered statistically significant at a P value of less than .05.

Results

Fischer's Ratio as a Predictive Factor for Treatment Response

The clinical characteristics of patients who received Peg-IFN and RBV combination therapy are shown in Table 1 and Supplementary Table 1, and explanations of these characteristics have been described previously.[4] All patients were infected with HCV genotype 1b and had a high viral load (>100 IU/mL). We compared patients with SVR + TR against those with NR, as assessed by the overall plausibility of treatment response groups using Fisher's C statistic as previously described.[4] We included data on the IL-28B polymorphism and plasma amino acid composition (aminogram).

Univariate regression analysis showed that no single amino acid was associated significantly with treatment response; however, using Fischer's ratio, the BCAA (Ile+Leu+Val)/aromatic amino acids (Phe+Tyr) ratio was associated significantly with treatment response (P = .005) (Table 1). Of the 121 patients with IL-28B major type, SVR, TR, and NR were observed in 53%, 37%, and 10%, respectively, and among 33 patients with IL-28B minor type, SVR, TR, and NR were observed in 15%, 17%, and 68%, respectively (P < .001) (data not shown). Fischer's ratio of SVR, TR, and NR was 2.35 ± 0.38, 2.30 ± 0.29, and 2.10 ± 0.31, respectively (P < .015) (data not shown).

We selected IL-28B polymorphism, hepatic ISG expression, fibrosis stage, HCV RNA, interferon sensitivity determining region mutation, and Fischer's ratio as factors for multivariate analysis. Multivariate analysis revealed that the minor type of IL-28B polymorphism (TG or GG at rs8099917) (odds ratio, 19.7; P < .001), advanced fibrosis stage of the liver (F3–4) (odds ratio, 6.35; P = .001), high hepatic ISGs (≧3.5) (odds ratio, 5.26; P = .005), low Fischer's ratio (continuous range, 1.5–3.3) (unit odds, 8.91; P = .011), and presence of ISDR mutation (≦1) (odds ratio, 4.12; P = .019) independently contributed to NR (Table 1).

The distribution of the Fischer's ratio according to fibrosis stage is shown in Supplementary Figure 1. The ratio decreased significantly in advanced fibrosis stage (F3–4) compared with early fibrosis stage (F1). No significant association between major or minor type of IL-28B polymorphism and different fibrosis stages of the liver was observed (Supplementary Figure 1*A*). In early fibrosis (F1–2) (Supplementary Figure 1*B*), 90% (80 of 89) of SVR+TR cases had the major type of IL-28B polymorphism, and 94% (16 of 17) of NR cases had the minor type. However, in the advanced fibrosis stage of the liver (F3–4) (Supplementary Figure 1*C*), 85% (23 of 27) of SVR+TR cases had the major type of IL-28B polymorphism and 50% (10 of 20) of NR cases had the minor type. Thus, in advanced fibrosis stages, factors other than the IL-28B polymorphism appear to contribute to NR. Interestingly, the Fischer's ratio was significantly lower in NR patients than SVR+TR pa-

tients in the advanced fibrosis stage of the liver. Therefore, Fischer's ratio could be an important predictor for NR that is independent of IL-28B polymorphism and histologic stage of the liver.

Fischer's Ratio and mTORC1 Signaling in CH-C Livers

Hepatic gene expression in 91 of 168 patients (Supplementary Table 1) was obtained using Affymetrix genechip analysis as described previously.[4] To examine the relationship between the plasma Fischer's ratio and mTORC1 signaling in the liver we evaluated the expression of key regulatory genes related to mTORC1 signaling. We found that expression of branched chain amino-acid transaminase 1 (BCAT1), an important catalytic enzyme of BCAA, was significantly negatively correlated with Fischer's ratio (Figure 1*A*). This indicates that the plasma Fischer's ratio is regulated in the liver as well as in peripheral muscle. Interestingly, the expression of c-myc, a positive regulator of BCAT1 (Figure 1*C*),[15] was correlated negatively with the Fischer's ratio (Figure 1*B*). The expression of PDCD4, a negative transcriptional target of ribosomal p70 S6 protein kinase (S6K), downstream of mTORC1, was correlated significantly with BCAT1 (Figure 1*D* and *E*). Thus, in CH-C livers, BCAT1 is induced with progressive liver disease and mTORC1 signaling is repressed, a process that might involve c-myc. Fischer's ratio of the plasma therefore can be seen to reflect mTORC1 signaling in the liver.

Impaired IFN Signaling in Huh-7 Cells Grown in Low-Amino-Acid Medium

Recent reports have shown the functional relevance of mTOR on IFN signaling and antiviral responses.[9,10] To evaluate IFN-alfa signaling and the mTOR pathway, we used Huh-7 cells grown in different amino acid conditions (×1 DMEM, ×1/5 DMEM, ×1/30 DMEM, and ×1/100 DMEM). The phosphorylated forms of mTOR (p-mTOR) and S6K (pS6K), an important downstream regulator of mTORC1 signaling, were decreased substantially in ×1/30 DMEM and ×1/100 DMEM (Figure 2*A*). Interestingly, the expression of the phosphorylated form of signal transducer and activator of transcription 1 (pSTAT1), an essential transducer of type 1 IFN signaling, also was decreased in these conditions (Figure 2*A*). Similarly, the expression of p-mTOR and pSTAT1 was repressed significantly in CH-C livers with a low Fischer's ratio compared with those with a high Fischer's ratio (Supplementary Figure 2, Supplementary Table 2).

To examine whether decreased pSTAT1 expression might be owing to repressed mTORC1 signaling, we knocked down the expression of Raptor, a specific subunit of mTORC1. We achieved more than 50% knockdown of Raptor by specific siRNA (Figure 2*B*). Under these conditions, the expression of p-mTOR and pSK6 were repressed, which is consistent with previous reports.[16] The expression of pSTAT1 also was repressed after Raptor knockdown (Figure 2*B*).

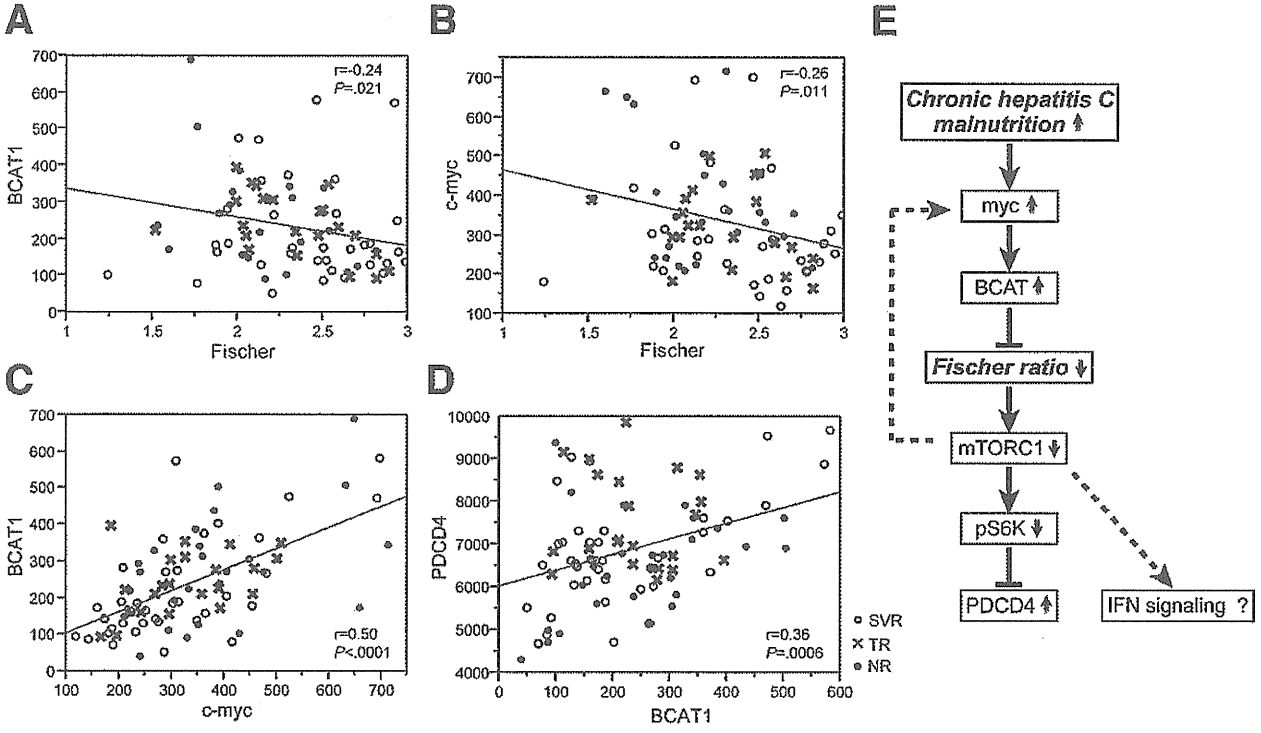

Figure 1. Regression analysis of mTORC1-related gene expression in liver. Gene expression values were determined by probe intensities. (*A*) BCAT1 and Fischer's ratio. (*B*) c-myc and Fischer's ratio. (*C*) BCAT1 and c-myc. (*D*) PDCD4 and BCAT1. (*E*) Putative signaling of mTORC1-related genes in CH-C.

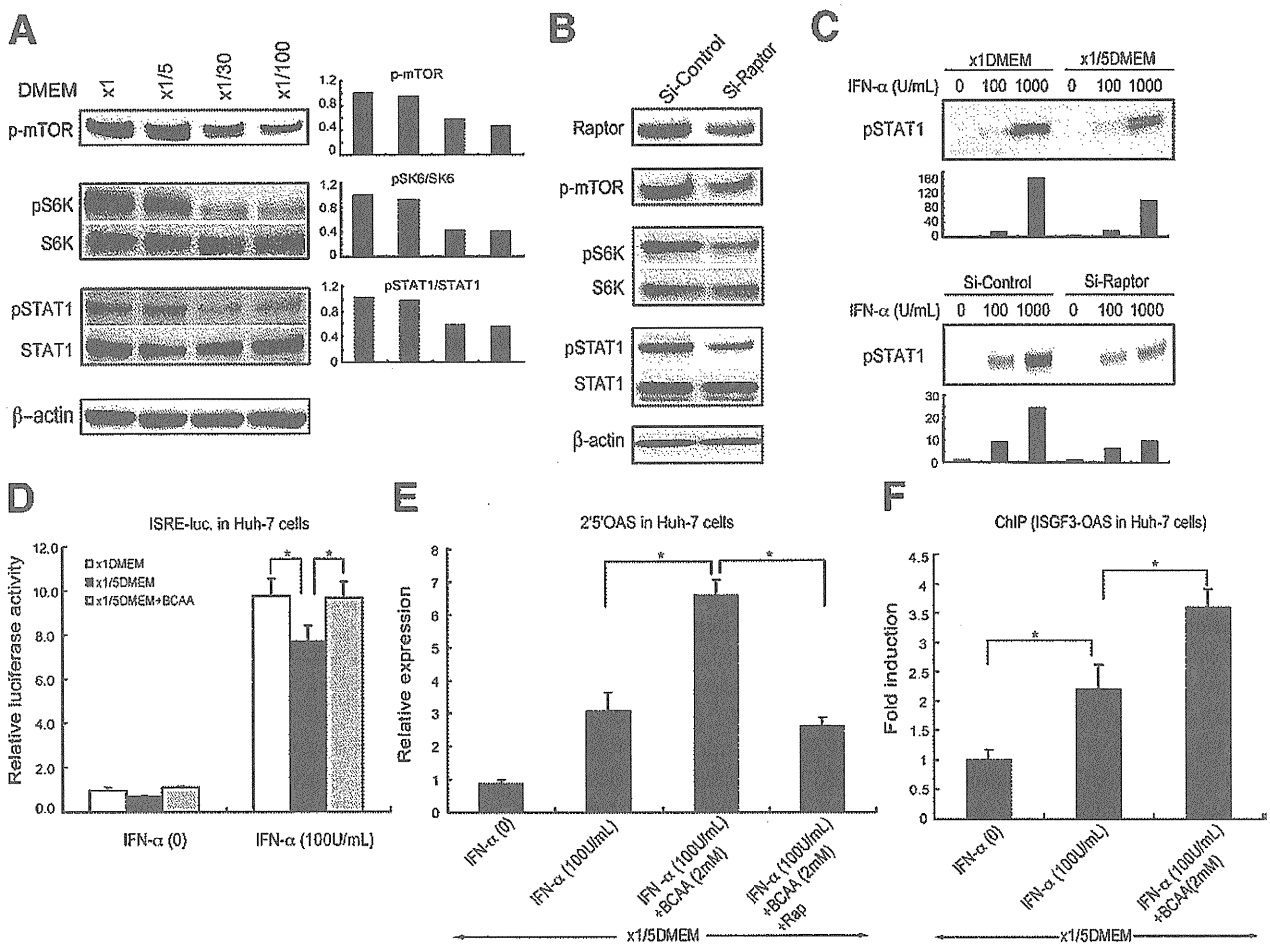

Figure 2. mTORC1 and IFN signaling in Huh-7 cells in low-amino-acid medium. (*A*) p-mTOR, pS6K, and pSTAT1 expression in different amino acid media. (*B*) p-mTOR, pS6K, and pSTAT1 expression under Raptor knock-down conditions. (*C*) IFN-alfa stimulation and pSTAT1 expression in low-amino-acid media or under Raptor knock-down conditions. (*D*) IFN-alfa stimulation and ISRE reporter activities in normal and low-amino-acid media. (*E*) IFN-alfa stimulation and 2'5'OAS expression supplemented with BCAA or rapamycin in low-amino-acid medium. (*F*) Chromatin immunoprecipitation of 2'5'OAS promoter region by ISGF3γ.

The induction of pSTAT1 by IFN-alfa (1000 U/mL) stimulation was impaired in ×1/5 DMEM or in Raptor knocked-down condition, compared with the control (Figure 2*C*). Consistent with these results, IFN-alfa–induced ISRE-dependent transcriptional activity, as measured using an ISRE-luciferase reporter assay, was impaired significantly in ×1/5 DMEM compared with ×1 DMEM (Figure 2*D*). However, this activity could be rescued by the addition of 2 mmol/L BCAA (Figure 2*D*). These results were confirmed by determining the expression of the endogenous IFN-alfa responsive gene, 2'5'OAS, using quantitative reverse-transcription PCR. Figure 2*E* shows that BCAA treatment augmented 2'5'OAS expression in low levels of amino acids, and that this could be reversed by the addition of rapamycin, an inhibitor of mTORC1 (Figure 2*E*). Furthermore, chromatin immunoprecipitation (ChIP) experiments revealed that transcriptional augmentation by BCAA was mediated by the binding of the IFN-alfa–inducible transcription factor, ISGF3γ, to the promoter region of 2'5'OAS (Figure 2*F*). These results indicate that amino acids in culture media play an essential role in IFN-alfa signaling through mTORC1 signaling, and that the addition of BCAA can overcome impaired IFN-alfa signaling in Huh-7 cells.

Induction of Socs3 in Low-Amino-Acid Medium in Huh-7 Cells

Besides being involved in mTOR signaling, Foxo transcriptional factors mediate another important branch of nutrition-sensing signaling pathway.[17] Therefore, we evaluated forkhead box O3A (Foxo3a) expression in low-amino-acid conditions in Huh-7 cells. After 6 hours culture in ×1/5, ×1/30, and ×1/100 DMEM, expression of the phosphorylated form of Foxo3a (pFoxo3a) decreased, whereas that of total Foxo3a increased in ×1/5 and ×1/30 DMEM, and the ratio of pFoxo3a to Foxo3a (pFoxo3a/Foxo3a) substantially decreased (Figure 3*A* and *B*). It has been reported that dephosphorylated Foxo3a is translocated to the nucleus before activation of its target genes.[18] In the present study, immunofluorescent staining

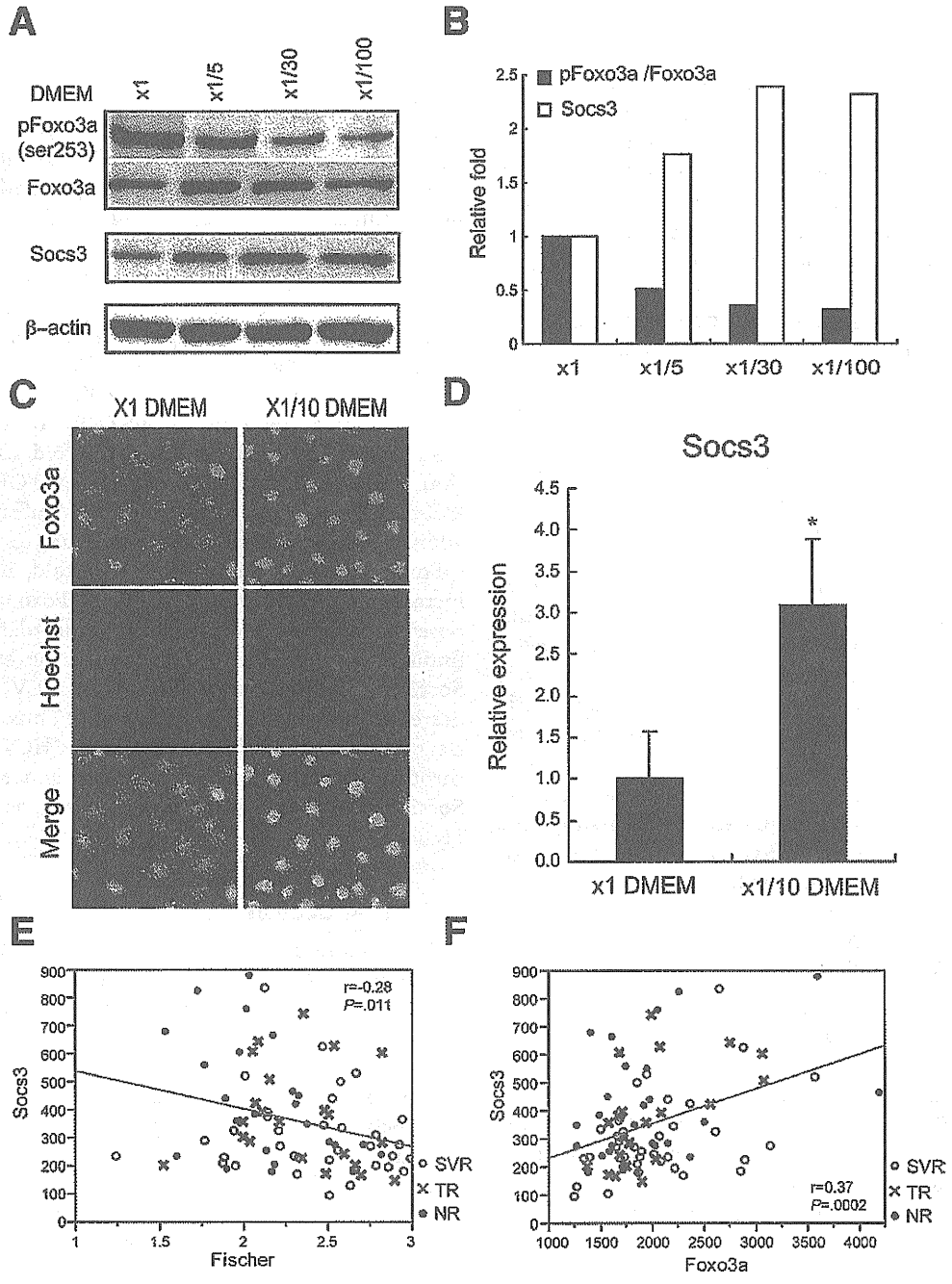

Figure 3. Foxo3a and Socs3 signaling in Huh-7 cells in low-amino-acid medium. (*A*) Foxo3a and Socs3 expression in different amino acid media. (*B*) Relative change of pFoxo3a/Foxo3a and Socs3 expression in different amino acid media. (*C*) Immunofluorescence staining of Foxo3a in Huh-7 cells in normal and low-amino-acid media. (*D*) Relative change of Socs3 messenger RNA in Huh-7 cells in normal and low-amino-acid media. (*E*) Regression analysis of Socs3 in liver and Fischer's ratio. (*F*) Regression analysis of Socs3 and Foxo3a in liver.

with an anti-Foxo3a antibody showed that Foxo3a diffused in both the cytoplasm and nucleus in normal amino acid medium, but localized in the nucleus in low-amino-acid medium (×1/10 DMEM) (Figure 3*C*).

Interestingly, in low-amino-acid medium, transcription and protein expression of Socs3 increased significantly (Figure 3*A*, *B*, and *D*). The induction of Socs3 in a state of malnutrition also was confirmed in clinical samples. In CH-C livers there was a significant negative correlation between the plasma Fischer's ratio and Socs3 expression, implying that Socs3 expression increases during the malnutrition state induced by CH-C. There was also a significant correlation between Foxo3a and the transcriptional level of Socs3 in CH-C livers (Figure 3*E* and *F*), suggesting an in vitro and in vivo biological role for Foxo3a in the activation of Socs3 expression. These findings also were confirmed by Western blotting of CH-C livers (Supplementary Figure 2, Supplementary Table 2).

Socs3 Is a Transcriptional Target of Foxo3a

The significant correlation between Socs3 and Foxo3a in CH-C livers prompted us to analyze the Socs3 promoter sequence and, in doing so, we identified a putative Foxo binding element (FBE) (Figure 4*A*). To investigate the functional relevance of Foxo3a in the transcriptional regulation of Socs3, we constructed reporter plasmids containing a luciferase coding region fused to the Socs3 promoter region (Socs3-luc). Socs3-luc promoter activity was increased substantially by the overexpression of Foxo3a (Figure 4*B*). The mutations introduced in the putative FBE (FBEmut) in the Socs3 promoter significantly reduced Foxo3a-induced Socs3 promoter activation (Figure 4*B*).

Foxo3a then was knocked down by siRNA and Socs3 induction was evaluated. After suppression of Foxo3a (Supplementary Figure 3), Socs3 promoter activity was repressed significantly in low-amino-acid medium (×1/10 DMEM) (Figure 4*C*). Thus, Foxo3a appears to be indispensable for activating the Socs3 promoter under low-amino-acid conditions. Correlating with these results, ChIP assays using an anti-Foxo3a antibody showed a significant increase in the association between Foxo3a and the FBE of the Socs3 promoter in low-amino-acid conditions (×1/10 DMEM) (Figure 4*D*). Taken together, these results suggest that, besides mTORC1 signaling, the Foxo3a-mediated Socs3 signaling pathway might contribute to impaired IFN signaling in a state of malnutrition in CH-C. BCAA potentially restores this signaling (Figure 4*E*).

Effect of BCAA on HCV Replication in Huh-7 or Huh-7.5 Cells

Based on the earlier-described results, we used 2 HCV in vitro replication systems to examine whether BCAA affects HCV replication in Huh-7 or Huh-7.5 cells. The first system used a recombinant infectious genotype 1a clone, H77S.3/GLuc2A (Supplementary Materials and Methods, Supplementary Figure 4), including reporter genes, whereas the second used continuously JFH-1–infecting Huh-7 cells (Supplementary Materials and Methods).

The synthetic RNA transcribed from pH77S.3/GLuc2A was introduced into Huh-7.5 cells and replication of H77S.3/GLuc2A was evaluated in normal or low-amino-acid medium supplemented with BCAA. H77S.3/GLuc2A increased significantly by 2.6-fold in Huh-7.5 cells grown in low-amino-acid medium (×1/5 DMEM) compared with normal amino acid medium (×1 DMEM). Interestingly, BCAA repressed H77S.3/GLuc2A replication in a dose-dependent manner (Figure 5*A*). In agreement with these results, the expression of Mx-1 was increased significantly by the addition of BCAA (Figure 5*B*). Similar findings were observed in JFH-1–infecting Huh-7 cells (Materials and Methods, Supplementary Figure 4). Although no obvious increase in HCV replication was observed in low-amino-acid medium (×1/5 DMEM) compared with normal amino acid medium (×1 DMEM), JFH-1 replication was repressed significantly by the addition of BCAA in a dose-dependent manner (Figure 5*D*). The expression of Mx-1 was increased substantially by the addition of BCAA (Figure 5*E*), suggesting that BCAA significantly repressed HCV replication in cells with either naive or persistent HCV infection. Importantly, there were no significant differences in cell viability between the conditions (Figure 5*C* and *F*).

To validate these findings, signaling pathways in HCV replicating cells were examined (Figure 6*A* and *B*). BCAA increased pS6K in a dose-dependent manner, implying its involvement in the activation of mTORC1 signaling. Related to this, expression of pSTAT1 was shown to be increased and the ratio of pSTAT1 to total STAT1 (pSTAT1/STAT1) increased 2.5- to 3-fold after the addition of BCAA. Thus, BCAA activated mTORC1 and the JAK-STAT signaling pathway in HCV-infected cells. In addition, the expression ratio of pFoxo3a to total Foxo3a (pFoxo3a/Foxo3a) increased 3- to 4-fold, indicating an increase in the cytoplasmic form of Foxo3a that is exposed to proteasome degradation. Concordant with these findings, we observed a decrease in the expression of Socs3. In addition, expression of the HCV core protein decreased as shown in Figure 6*A* and *B*. Thus, these results clearly show that BCAA repressed HCV replication through activation of IFN signaling and repression of Socs3-mediated IFN inhibitory signaling, as proposed in Figure 4*E*.

Discussion

Thompson et al[5] showed that the IL-28B polymorphism, HCV RNA, nationality (Caucasian/Hispanic vs African American), hepatic fibrosis stage, and fasting blood sugar level are all significant variables for achieving SVR in patients infected with genotype 1 HCV. However, the significance of variable factors for treatment response in conjunction with the IL-28B polymorphism has not been evaluated fully. In the present study, in addition to previously examined variables,[4] we included the plasma Fischer's ratio as a nutritional parameter. Multivariate analysis showed that the minor type of IL-28B polymorphism, advanced fibrosis stage, high hepatic ISGs, low Fischer's ratio, and ISDR mutation (≤1) independently contributed to NR (Table 1). Interestingly, among patients of similar fibrosis stage (F3–4), the Fischer's ratio was significantly lower in NR than SVR+TR cases. Therefore, the plasma value of Fischer's ratio was associated with the treatment response that was independent of the IL-28B polymorphism and histologic stage of the liver, although patients with advanced hepatic fibrosis are likely to be nutritionally affected.

As a nutrient sensor signaling pathway, the protein kinase mTOR plays an essential role in maintaining homeostasis and regulates protein synthesis in response to nutrient conditions. mTOR is the catalytic subunit of 2 distinct complexes, mTORC1 and mTORC2. In addition

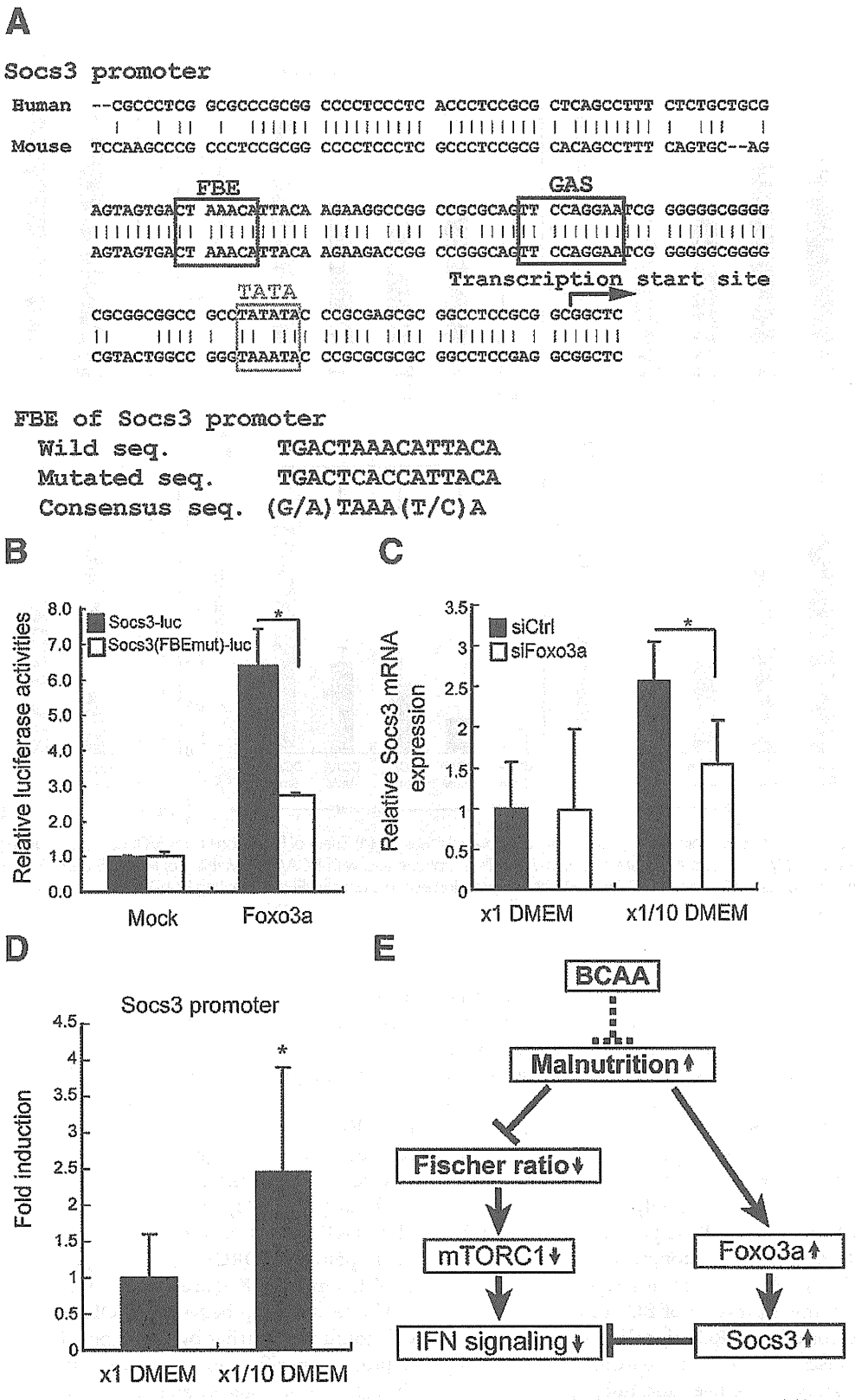

Figure 4. Socs3 promoter assay. (*A*) Primary structure of putative Foxo binding element in Socs3 promoter region. (*B*) Socs3-luc and Socs3 (FBEmut)-luc activities after overexpression of Foxo3a in Huh-7 cells. (*C*) Relative Socs3 messenger RNA (mRNA) expression after knockdown of Foxo3a in normal and low-amino-acid media. (*D*) Chromatin immunoprecipitation of Socs3 promoter region by Foxo3a in normal and low-amino-acid media. (*E*) Model of impaired IFN signaling by repressed mTORC1 signaling and increased Socs3 signaling under CH-C state of malnutrition.

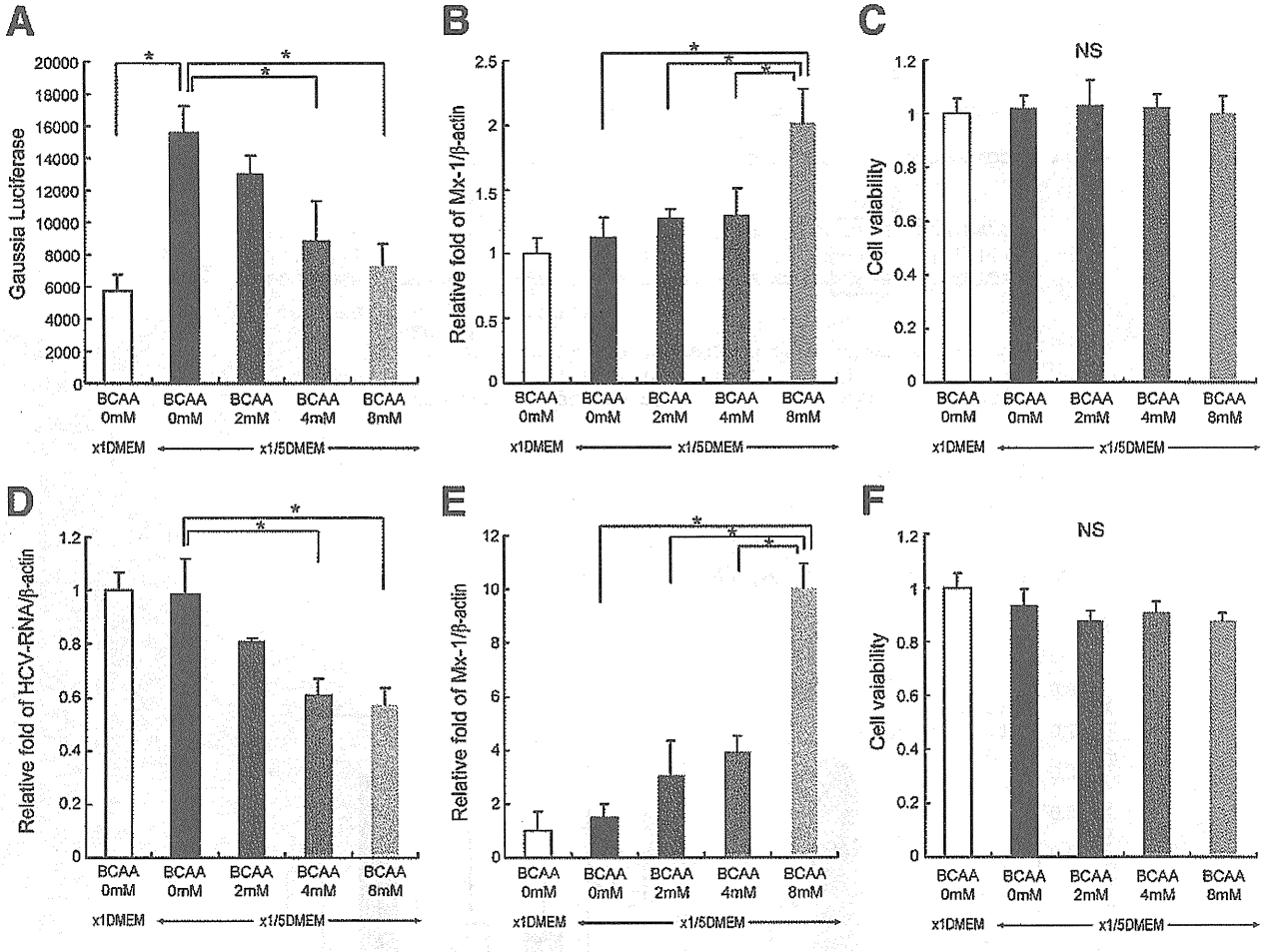

Figure 5. Effect of BCAA on HCV replication in cells in low-amino-acid medium. (*A*) Effect of BCAA on H77S.3/GLuc2A replication in Huh-7.5 cells. (*B*) Mx-1 expression in H77S.3/GLuc2A-transfected Huh-7.5 cells supplemented with BCAA. (*C*) Viability of Huh-7.5 cells. (*D*) Effect of BCAA on JFH-1 replication continuously infecting Huh-7 cells. (*E*) Mx-1 expression in continuously JFH-1–infecting Huh-7 cells supplemented with BCAA. (*F*) Viability of Huh-7 cells.

to these metabolic aspects, recent reports have shown that mTORC1 participates in IFN signaling and antiviral defense responses,[9,10] although the precise signaling pathway has not yet been clarified. In the present study, we evaluated mTORC1 signaling in CH-C livers using gene expression profiling of 91 patients (Figure 1, Supplementary Table 1). We observed a significant negative correlation between plasma Fischer's ratio and hepatic expression of BCAT1, an important catalytic enzyme of BCAA (Figure 1*A*). Moreover, BCAT1 expression was correlated positively with PDCD4 expression, which in turn is regulated negatively by pS6K at the transcriptional level (Figure 1*D*).[16] Thus, the expression of BCAT1 appears to be a negative indicator of mTORC1 signaling in the liver, and the plasma Fischer's ratio is partially reflected by mTORC1 signaling in the liver and muscle.

Interestingly, the expression of c-myc was correlated significantly with BCAT1 (Figure 1*C*) as reported previously.[15] Several studies observed up-regulated c-myc expression in advanced stages of CH-C[19] but, on the other hand, c-myc recently was shown to be a target of mTORC1 in hepatic cells.[17] The existence of a feedback mechanism between c-myc and mTORC1 signaling to maintain liver homeostasis (Figure 1*E*) is plausible, although the precise mechanisms need to be confirmed.

Impaired mTORC1 signaling is suggested to affect the IFN-alfa–induced signaling pathway. To address this, the relationship between mTORC1 and IFN signaling was assessed using a cell culture system. In low-amino-acid medium (×1/5, ×1/30, and ×1/100 DMEM), expression of pSTAT1 was decreased substantially, correlating with the impaired mTORC1 signaling represented by decreased p-mTOR and pS6K expression in Huh-7 cells (Figure 2*A*).

The relationship between mTORC1 and IFN signaling was confirmed further by the knock-down experiment of Raptor, a specific subunit of mTORC1 (Figure 2*B*), although a more precise analysis should be performed to confirm this relationship. Importantly, when Huh-7 cells were stimulated by IFN-alfa, pSTAT1 induction was repressed significantly in low-amino-acid medium (×1/5 DMEM) or in Raptor knocked-down conditions (Figure 2*C*). It therefore could be speculated that IFN treat-

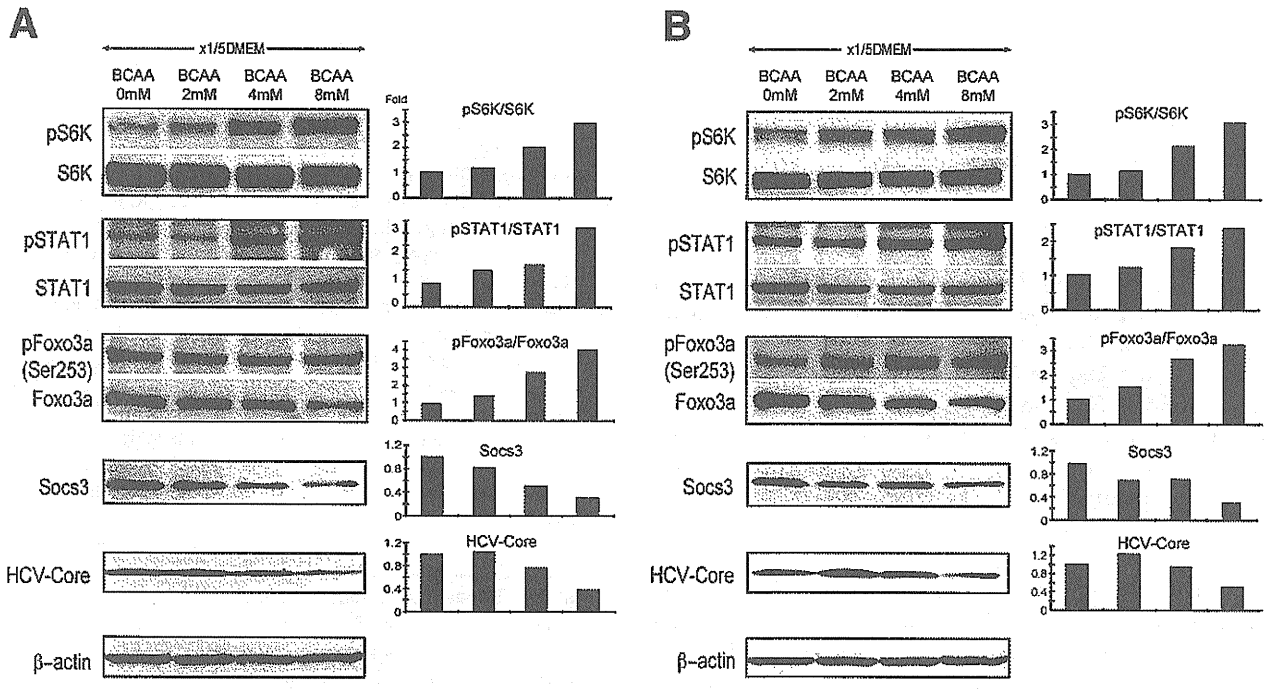

Figure 6. Expression of S6K, STAT1, Foxo3a, Socs3, and HCV core in H77S.3/GLuc2A-transfected Huh-7.5 cells or continuously JFH-1–infecting Huh-7 cells supplemented with BCAA.

ment of patients with liver malnutrition and impaired mTORC1 signaling would lead to reduced induction of ISGs. Importantly, BCAA was able to restore impaired IFN signaling through increased binding of ISGF3γ to its targets (Figure 2*D–F*).

Besides cross-talk of mTORC1 and IFN signaling, we revealed that Foxo3a also is involved in the IFN inhibitory pathway. In low-amino-acid medium, expression of pFoxo3a (ser253) was decreased substantially whereas that of Socs3 was increased. A decreased pFoxo3a/Foxo3a ratio indicates nuclear accumulation of Foxo3a before activation of its target genes, and this was confirmed by immunofluorescent staining (Figure 3*C*). The expression of Foxo3a was significantly positively correlated with that of Socs3 in CH-C liver (Figure 3*F*). These findings prompted us to identify a putative FBE in the Socs3 promoter region (Figure 4*A*). In fact, Socs3 promoter reporter activity was activated by overexpression of Foxo3a, and mutation of FBE impaired Foxo3a-dependent Socs3 promoter activation. Conversely, induction of Socs3 was not observed when expression of Foxo3a was knocked down by siRNA in low-amino-acid medium. Socs3 induction in low-amino-acid medium was owing to increased binding of Foxo3a to the FBE, which was confirmed by ChIP (Figure 4*D*). Therefore, in addition to impaired mTORC1 signaling, the Foxo3a-mediated Socs3 IFN inhibitory pathway might be involved in impaired IFN signaling in patients with liver malnutrition (Figure 4*E*).

Finally, we examined whether BCAA could restore impaired IFN signaling and inhibit HCV replication in cells under conditions of malnutrition. Importantly, BCAA could repress replication of the recombinant genotype 1a-derived HCV, H77S.3/GLuc2A, in a dose-dependent manner (Figure 5*A*). H77S.3/GLuc2A RNA produces infectious virus[14] and, therefore, the results indicate that BCAA might act on a naive HCV infection. Moreover, BCAA inhibited JFH-1–infected Huh-7 cells in which JFH-1 continuously was infecting in a dose-dependent manner. These results indicate that BCAA had an inhibitory effect on either naive or persistent HCV infection irrespective of genotypes (1a and 2a). Consistent with these results, BCAA induced the expression of pSTAT1 and Mx protein in a dose-dependent manner, and repressed Socs3 expression through increasing the ratio of pFoxo3a (ser243) to Foxo3a in a dose-dependent manner (Figures 5 and 6). Therefore, BCAA potentially could restore impaired IFN signaling and inhibit HCV replication in a CH-C state of malnutrition.

In conclusion, we addressed the clinical significance of the nutritional state of the liver on the treatment response of Peg-IFN and RBV combination therapy for CH-C. Although further studies are required to fully define the precise mechanisms underlying mTOR and IFN signaling, we showed that plasma values of Fischer's ratio are a useful nutritional parameter associated with treatment response. Fischer's ratio reflects mTORC1 signaling in the liver, which is correlated with IFN signaling and related to Socs3 IFN inhibitory signaling through Foxo3a. The potential usefulness of BCAA for the augmentation of IFN signaling could suggest a new therapeutic application for advanced-stage CH-C.

Supplementary Material

Note: To access the supplementary material accompanying this article, visit the online version of *Gastroenterology* at www.gastrojournal.org, and at doi: 10.1053/j.gastro.2011.03.051.

Appendix A

The Hokuriku Liver Study Group is composed of the following members: Drs Takashi Kagaya, Kuniaki Arai, Kaheita Kakinoki, Kazunori Kawaguchi, Hajime Takatori, and Hajime Sunakosaka (Department of Gastroenterology, Kanazawa University Graduate School of Medicine, Kanazawa, Japan); Drs Touru Nakahama and Shinji Kamiyamamoto (Kurobe City Hospital, Kurobe, Toyama, Japan); Dr Yasuhiro Takemori (Toyama Rosai Hospital, Uozu, Toyama, Japan); Dr Hikaru Oguri (Koseiren Namerikawa Hospital, Namerikawa, Toyama, Japan); Drs Yatsugi Noda and Hidero Ogino (Toyama Prefectural Central Hospital, Toyama, Japan); Drs Yoshinobu Hinoue and Keiji Minouchi (Toyama City Hospital, Toyama, Japan); Dr Nobuyuki Hirai (Koseiren Takaoka Hospital, Takaoka, Toyama, Japan); Drs Tatsuho Sugimoto and Koji Adachi (Tonami General Hospital, Tonam, Toyama, Japan); Dr Yuichi Nakamura (Noto General Hospital, Nanao, Ishikawa, Japan); Drs Masashi Unoura and Ryuhei Nishino (Public Hakui Hospital, Hakui, Ishikawa, Japan); Drs Hideo Morimoto and Hajime Ohta (National Hospital Organization Kanazawa Medical Center, Kanazawa, Ishikawa, Japan); Dr Hirokazu Tsuji (Kanazawa Municipal Hospital, Kanazawa, Ishikawa, Japan); Drs Akira Iwata and Shuichi Terasaki (Kanazawa Red Cross Hospital, Kanazawa, Ishikawa, Japan); Drs Tokio Wakabayashi and Yukihiro Shirota (Saiseikai Kanazawa Hospital, Kanazawa, Ishikawa, Japan); Drs Takeshi Urabe and Hiroshi Kawai (Public Central Hospital of Matto Ishikawa, Hakusan, Ishikawa, Japan); Dr Yasutsugu Mizuno (Nomi Municipal Hospital, Nomi, Ishikawa, Japan); Dr Shoni Kameda (Komatsu Municipal Hospital, Komatsu Ishikawa, Japan); Drs Hirotoshi Miyamori and Uichiro Fuchizaki (Keiju Medical Center, Nanao, Ishikawa, Japan); Dr Haruhiko Shyugo (Kanazawa Arimatsu Hospital, Kanazawa, Ishikawa, Japan); Dr Hideki Osaka (Yawata Medical Center, Komatsu, Ishikawa, Japan); Dr Eiki Matsushita (Kahoku Central Hospital, Tsubata, Ishikawa, Japan); Dr Yasuhiro Katou (Katou Hospital, Komatsu, Ishikawa, Japan); Drs Nobuyoshi Tanaka and Kazuo Notsumata (Fukuiken Saiseikai Hospital, Fukui, Japan); Dr Mikio Kumagai (Kumagai Clinic, Tsuruga, Fukui, Japan); and Dr Manabu Yoneshima (Municipal Tsuruga Hospital, Tsuruga, Fukui, Japan).

References

1. Fried MW, Shiffman ML, Reddy KR, et al. Peginterferon alfa-2a plus ribavirin for chronic hepatitis C virus infection. N Engl J Med 2002;347:975–982.
2. Tanaka Y, Nishida N, Sugiyama M, et al. Genome-wide association of IL28B with response to pegylated interferon-alpha and ribavirin therapy for chronic hepatitis C. Nat Genet 2009;41: 1105–1109.
3. Ge D, Fellay J, Thompson AJ, et al. Genetic variation in IL28B predicts hepatitis C treatment-induced viral clearance. Nature 2009;461:399–401.
4. Honda M, Sakai A, Yamashita T, et al. Hepatic ISG expression is associated with genetic variation in interleukin 28B and the outcome of IFN therapy for chronic hepatitis C. Gastroenterology 2010;139:499–509.
5. Thompson AJ, Muir AJ, Sulkowski MS, et al. Interleukin-28B polymorphism improves viral kinetics and is the strongest pretreatment predictor of sustained virologic response in genotype 1 hepatitis C virus. Gastroenterology 2010;139:120–129 e18.
6. Nishitani S, Ijichi C, Takehana K, et al. Pharmacological activities of branched-chain amino acids: specificity of tissue and signal transduction. Biochem Biophys Res Commun 2004;313:387–389.
7. Matsumura T, Morinaga Y, Fujitani S, et al. Oral administration of branched-chain amino acids activates the mTOR signal in cirrhotic rat liver. Hepatol Res 2005;33:27–32.
8. Kim DH, Sarbassov DD, Ali SM, et al. mTOR interacts with raptor to form a nutrient-sensitive complex that signals to the cell growth machinery. Cell 2002;110:163–175.
9. Colina R, Costa-Mattioli M, Dowling RJ, et al. Translational control of the innate immune response through IRF-7. Nature 2008;452: 323–328.
10. Kaur S, Lal L, Sassano A, et al. Regulatory effects of mammalian target of rapamycin-activated pathways in type I and II interferon signaling. J Biol Chem 2007;282:1757–1768.
11. Shimbo K, Kubo S, Harada Y, et al. Automated precolumn derivatization system for analyzing physiological amino acids by liquid chromatography/mass spectrometry. Biomed Chromatogr 2009; 24:683–691.
12. Shirasaki T, Honda M, Mizuno H, et al. La protein required for internal ribosome entry site-directed translation is a potential therapeutic target for hepatitis C virus replication. J Infect Dis 2010;202:75–85.
13. Yi M, Villanueva RA, Thomas DL, et al. Production of infectious genotype 1a hepatitis C virus (Hutchinson strain) in cultured human hepatoma cells. Proc Natl Acad Sci U S A 2006;103:2310–2315.
14. Shimakami T, Welsch C, Yamane D, et al. Protease inhibitor-resistant hepatitis C virus mutants with reduced fitness from impaired production of infectious virus. Gastroenterology 2011; 140:667–675.
15. Eden A, Simchen G, Benvenisty N. Two yeast homologs of ECA39, a target for c-Myc regulation, code for cytosolic and mitochondrial branched-chain amino acid aminotransferases. J Biol Chem 1996; 271:20242–2045.
16. Dowling RJ, Topisirovic I, Alain T, et al. mTORC1-mediated cell proliferation, but not cell growth, controlled by the 4E-BPs. Science 2010;328:1172–1176.
17. Teleman AA, Hietakangas V, Sayadian AC, et al. Nutritional control of protein biosynthetic capacity by insulin via Myc in Drosophila. Cell Metab 2008;7:21–32.
18. Zhang X, Gan L, Pan H, et al. Phosphorylation of serine 256 suppresses transactivation by FKHR (FOXO1) by multiple mechanisms. Direct and indirect effects on nuclear/cytoplasmic shuttling and DNA binding. J Biol Chem 2002;277: 45276–45284.
19. Farinati F, Cardin R, Bortolami M, et al. Oxidative damage, pro-inflammatory cytokines, TGF-alpha and c-myc in chronic HCV-related hepatitis and cirrhosis. World J Gastroenterol 2006;12: 2065–2069.

Received October 19, 2010. Accepted March 18, 2011.

Reprint requests

Address requests for reprints to: Shuchi Kaneko, MD, PhD, Department of Gastroenterology, Graduate School of Medicine, Kanazawa University, Takara-Machi 13-1, Kanazawa 920-8641, Japan. e-mail: skaneko@m-kanazawa.jp; e-mail: fax: (81) 76-234-4250.

Acknowledgments

Participating investigators from the Hokuriku Liver Study Group are listed in Appendix A.

The authors thank Mina Nishiyama and Yuki Hatayama for excellent technical assistance.

Conflicts of interest

The authors disclose no conflicts.

Supplementary Materials and Methods

Plasma Amino Acid Analysis

Plasma sample amino acid concentrations were measured by high-performance liquid chromatography–electrospray ionization–mass spectrometry followed by derivatization.[1] An MSQ Plus LC/MS system (Thermo Fischer Scientific, Waltham, MA) equipped with an electrospray ionization source was used in positive ionization mode for selected ion monitoring. Xcalibur version 1.4 SR1 software (Thermo Fischer Scientific, Yokohama, Japan) was used for data collection and processing. The high-performance liquid chromatography separation system consisted of an L-2100 pump, L-2200 autosampler, and L-2300 column oven (Hitachi High-Technologies Corporation, Tokyo, Japan). A Wakosil-II 3C8-100HG column (100, 2.1, 3 mm; Wako Pure Chemical Industries, Osaka, Japan) was used for the separation, and the mobile phase consisted of eluent A (25-mmol/L ammonium formate in water, pH 6.0) and eluent B (water:acetonitrile = 40:60).

Western Blotting

The expression of HCV core protein, Socs3, Foxo3a, phospho-Foxo3a (Ser253) (pFoxo3a), STAT1, pSTAT1 (Tyr701), S6K, pS6K, p-mTOR (Ser2448), Raptor, and β-actin were evaluated with mouse anti-core (Affinity BioReagents, Golden, CO), mouse anti-Socs3 (Santa Cruz Biotechnology, Santa Cruz, CA), rabbit anti-Foxo3a, rabbit anti-β-actin (Sigma-Aldrich, St Louis, MO), rabbit anti-phospho-Foxo3a (Ser253), rabbit anti-STAT1, rabbit anti-p-STAT1 (Tyr701), rabbit anti-p70 S6K, rabbit anti-pS6K, rabbit anti-p-mTOR (Ser2448), and rabbit anti-Raptor (Cell Signaling Technology, Beverly, MA), respectively. Densitometric analysis was conducted directly on the blotted membrane using a charge coupled device camera system (LAS-3000 Mini; Fujifilm, Tokyo, Japan) and Scion Image software (Frederick, MD).

Primer Sequences for PCR and siRNA

Primer sequences for PCR and siRNA were as follows: 2′5′OAS: forward 5′- CTC AGA AAT ACC CCA GCC AAA TC-3′, reverse 5′-GTG GTG AGA GGA CTG AGG AA-3′; Socs3: forward 5′-TAC CAC CTG AGT CTC CAG CTT CTC-3′, reverse 5′-CCT GGC AGT TCT CAT TAG TTC AGC ATT C-3′; Foxo3a: forward 5′-TGC TGT ATG CAA GAA CTT TCC AGT AGC AG-3′, reverse 5′-ACT CTA GCC CCC ATG CTA CTA GTG-3′; glyceraldehyde-3-phosphate dehydrogenase: forward 5′-GAA GGT GAA GGT CGG AGT-3′, reverse 5′-GAA GAT GGT GAT GGG ATT TC-3′, siFoxo3a (SASI_Hs01_00119127; Sigma) sense: 5′-GAA UGA UGG GCU GAC UGA AdTdT-3′, antisense: 5′-UUC AGU CAG CCC AUC AUU CdTdT-3′. Small interfering Raptor was purchased as part of KIAA1303 siGENOME SMART pool siRNA reagents from Dharmacon, Inc (Lafayette, CO).

Construction of ISRE-Luc Reporter and FBEmut-luc Reporter Plasmids

Oligonucleotides containing the ISRE tandem repeat sequence (sense 5′-TCG AGA ACT GAA ACT GAA ACT GAA ACT GAA ACT GAA ACT GAA ACT GAA ACT GAA A-3′, antisense 5′-AGC TTT TCA GTT TCA GTT TCA GTT TCA GTT TCA GTT TCA GTT TCA GTT TCA GTT C-3′, consensus 5′-GAA Ann GAA ACT-3′) were annealed, and integrated into Xho I and Hind III sites of the pGL4.23 luciferase vector (Promega). The human Socs3 promoter region (-109/+217) was amplified by genomic PCR using specific primers (forward, 5′-TGC TGC GAG TAG TGA CTA AAC ATT ACA AG-3′ and reverse, 5′-CCG TGA AGT CCA CAA AGG AGC CTT C-3′) and cloned into the EcoR V site of the pGL4.10-luc2 reporter vector (Promega). The Socs3 FBE mutant reporter vector was created by substituting 2 adenines in the putative FBE with guanines (wild-type sequence 5′-CTAAACA-3′, mutated sequence 5′-CTGAGCA-3′).

ChIP Assay

For the ChIP assay using the anti-ISGF3γ antibody, 1×10^6 Huh-7 cells were treated with IFN-alfa (0 or 100 U/mL) and BCAA (2 mmol/L) in low-amino-acid medium for 6 hours. For ChIP using the anti-Foxo3a antibody, 1×10^6 Huh-7 cells were cultured in low-amino-acid medium for 24 hours.

Cells were cross-linked with 1% formaldehyde in PBS for 10 minutes at 37°C, and the reaction was stopped with 250 mmol/L glycine for 10 minutes. Cells were suspended in sodium dodecyl sulfate–lysis buffer (1% sodium dodecyl sulfate, 10 mmol/L ethylenediaminetetraacetic acid [EDTA], 50 mmol/L Tris-HCl [pH 8.1]), complete protease inhibitor cocktail (Roche Applied Science), and incubated for 30 minutes at 10°C. Cell lysate was sonicated with Bioruptor (Cosmo Bio, Tokyo, Japan) to obtain chromatin fragments and diluted 10-fold in ChIP dilution buffer (0.01% sodium dodecyl sulfate, 1.1% Triton-X 100, 1.2 mmol/L EDTA, 16.7 mmol/L Tris-HCl [pH 8.1], 150 mmol/L NaCl, complete protease inhibitor cocktail). Chromatin fragments were incubated with 2 μg ISGF3γ antibody (Santa Cruz Biotechnology), 2 μg Foxo3a antibody (H-144; Santa Cruz Biotechnology), or normal rabbit immunoglobulin G for 18 hours at 4°C. Dynabeads (30 μL) protein G (Invitrogen) was added and incubated for 1 hour at 4°C. The beads were washed with low-salt-wash buffer (0.1% sodium dodecyl sulfate, 1% Triton-X 100, 2.0 mmol/L EDTA, 20 mmol/L Tris-HCl [pH 8.1], 150 mmol/L NaCl), high-salt-wash buffer (0.1% sodium dodecyl sulfate, 1% Triton-X 100, 2.0 mmol/L EDTA, 20 mmol/L Tris-HCl [pH 8.1], 500 mmol/L NaCl), LiCl wash buffer (250 mmol/L LiCl, 1% NP-40, 1% de-

oxycholate, 1.0 mmol/L EDTA, 1.0 mmol/L Tris-HCl [pH 8.1]) and Tris-EDTA buffer. Immunoprecipitated chromatin fragments were eluted with elution buffer (1% sodium dodecyl sulfate, 100 mmol/L NaHCO3, 10 mmol/L dithiothreitol), and reverse cross-linked by incubating for 6 hours at 65°C in elution buffer containing 200 mmol/L NaCl. DNA fragments were purified and quantified by real-time detection PCR with primers for putative ISRE in the 2′5′OAS promoter region (forward, 5′-AAA TGC ATT TCC AGA GCA GAG TTC AGA G-3′, reverse, 5′-GGG TAT TTC TGA GAT CCA TCA TTG ACA GG-3′) or putative FBE in the Socs3 promoter region (forward, 5′-TGC TGC GAG TAG TGA CTA AAC ATT ACA AG -3′, reverse, 5′-AGC GGA GCA GGG AGT CCA AGT C -3′). Values were normalized by the measurement of input DNA.

pH77S.3/GLuc2A

pH77S.2 is a modification of pH77S[2] containing an additional mutation within the E2 protein (N476D in the polyprotein) that promotes infectious virus yields from RNA-transfected cells (Yi et al, unpublished data). To monitor replication, the GLuc sequence, fused at its C terminus to the foot-and-mouth disease virus 2A autoprotease, was inserted between p7 and NS2 of pH77S.2 (Supplementary Figure 4). To insert the GLuc-coding sequence between p7 and NS2 in pH77S.2, followed by the foot-and-mouth disease virus 2A protein-coding sequence, Mlu I, EcoR V, and Spe I restriction sites were created between the p7 and NS2 coding sequences by site-directed mutagenesis. DNA coding for GLuc was subcloned into the Mlu I and EcoR V sites of the modified plasmid after PCR amplification using the primers: 5′- ATA ATA TTA CGC GTA *TGG GAG TCA AAG TTC TGT TTG CC*-3′ (sequence corresponding to the N-terminal GLuc is italicized and that corresponding to Mlu I is underlined) and 5′-ATA AAT AGAT ATC *GTC ACC ACC GGC CCC CTT GAT CTT*-3′ (C terminal GLuc is italicized and EcoR V is underlined). A DNA fragment encoding the 17 amino acids of the foot-and-mouth disease virus 2A protein was generated by annealing the following complementary oligonucleotides: 5′- ATA TGA TAT CAA CTT TGA CCT TCT CAA GTT GGC CGG CGA CGT CGA GTC CAA CCC AGG GCC CAC TAG CAT AT-3′ and 5′-ATA TGC TAG TGG GCC CTG GGT TGG ACT CGA CGT CGC CGG CCA ACT TGA GAA GGT CAA AGT TGA TAT CAT AT-3′ (underlined sequences indicate EcoR V and Spe I sites). The annealed oligonucleotides were digested by both restriction enzymes and the product inserted into the corresponding sites of pH77S.2 containing GLuc to generate pH77S.2/GLuc2A. Q41R is a cell-culture adaptive mutation within the NS3 protease domain of pH77S. Because it is not essential for production of infectious virus (Yi et al, unpublished data), pH77S.2 and pH77S.2/GLuc2A constructs underwent this mutation by site-directed mutagenesis of a PCR fragment spanning the Afe I and BsrG I sites to replace Gln_{41} with wild-type Arg. The resulting plasmids (pH77S.2/R41Q and pH77S.2/GLuc2A/R41Q) were redesignated pH77S.3 and pH77S.3/GLuc2A, respectively.[3,4] GLuc has several advantages over other luciferase reporter enzymes in that it is smaller and allows more sensitive detection than either firefly or Renilla luciferase.[3,4] In addition, a signal sequence directs its secretion into cell-culture media, allowing real-time dynamic measurements of GLuc expression without the need for cell lysis. H77S.3/GLuc2A RNA produces infectious virus, although with lower efficiency than H77S.3 RNA (10-fold less).

References

1. Shimbo K, Kubo S, Harada Y, et al. Automated precolumn derivatization system for analyzing physiological amino acids by liquid chromatography/mass spectrometry. Biomed Chromatogr 2009; 24:683–691.
2. Yi M, Villanueva RA, Thomas DL, et al. Production of infectious genotype 1a hepatitis C virus (Hutchinson strain) in cultured human hepatoma cells. Proc Natl Acad Sci U S A 2006;103:2310–2315.
3. Shetty S, Kim S, Shimakami T, et al. Hepatitis C virus genomic RNA dimerization is mediated via a kissing complex intermediate. RNA 2010;16:913–925.
4. Shimakami T, Welsch C, Yamane D, et al. Protease inhibitor-resistant hepatitis C virus mutants with reduced fitness from impaired production of infectious virus. Gastroenterology 2011; 140:667–675.

Biochemical and Biophysical Research Communications 407 (2011) 135–140

Contents lists available at ScienceDirect

Biochemical and Biophysical Research Communications

journal homepage: www.elsevier.com/locate/ybbrc

Hepatitis C virus RNA replication in human stellate cells regulates gene expression of extracellular matrix-related molecules

Noriyuki Watanabe [a], Hideki Aizaki [a], Tomokazu Matsuura [b], Soichi Kojima [c], Takaji Wakita [a,*], Tetsuro Suzuki [d]

[a] Department of Virology II, National Institute of Infectious Diseases, Tokyo, Japan
[b] Department of Laboratory Medicine, The Jikei University School of Medicine, Tokyo, Japan
[c] Molecular Ligand Biology Research Team, Chemical Genomics Group, Chemical Biology Department, RIKEN Advanced Science Institute, Saitama, Japan
[d] Department of Infectious Diseases, Hamamatsu University School of Medicine, Hamamatsu, Japan

ARTICLE INFO

Article history:
Received 19 February 2011
Available online 1 March 2011

Keywords:
HCV
Stellate cells
Fibrosis
Replicon cells

ABSTRACT

Hepatitis C virus (HCV) infection is a major cause of chronic liver disease, including chronic hepatitis, fibrosis, and cirrhosis. Fibrosis often develops in HCV-infected livers and ultimately leads to cirrhosis and carcinoma. During fibrosis, hepatic stellate cells (HSC) play important roles in the control of extracellular matrix synthesis and degradation in fibrotic livers. In this study, we established a subgenomic replicon (SGR) cell line with human hepatic stellate cells to investigate the effect of HCV RNA replication on HSC. Isolated SGR clones contained HCV RNA copy numbers ranging from 10^4 to 10^7 per μg total RNA, and long-term culture of low-copy number SGR clones resulted in markedly increased HCV RNA copy numbers. Furthermore, HCV RNA replication affected gene expression of extracellular matrix-related molecules in both hepatic stellate cells and hepatic cells, suggesting that HCV RNA replication and/or HCV proteins directly contribute to liver fibrosis. The HCV RNA-replicating hepatic stellate cell line isolated in this study will be useful for investigating hepatic stellate cell functions and HCV replication machinery.

1. Introduction

Hepatitis C virus (HCV) infection is a major cause of chronic liver disease, including chronic hepatitis, fibrosis, and cirrhosis, with greater than 170 million individuals infected worldwide [1,2]. Presently, there is no preventive vaccine for HCV infection, and standard therapy involves the combination of pegylated interferon-alpha and ribavirin [3]. However, as the effects of this combination therapy approach are often insufficient to completely eliminate viruses from HCV carriers, novel antiviral therapies are desired to increase sustained virological response rates and reduce adverse effects.

Fibrosis is often observed in chronic HCV infections and is part of the dynamic process of extracellular matrix (ECM) remodeling that occurs continuously during chronic liver injury. Such remodeling results in excessive accumulation of ECM proteins, ultimately leading to cirrhosis and carcinoma [4,5]. Hepatic stellate cells are the main collagen- and ECM-producing cells and play a key role in liver fibrogenesis [6]. In liver tissue, the balance between ECM synthesis and degradation is regulated by gene expression of ECM-regulatory molecules, such as matrix metalloproteinases (MMP) and tissue inhibitors of matrix metalloproteinase (TIMP). On activation of hepatic stellate cells by inflammatory molecules, the balance of ECM regulation shifts towards progression of liver fibrosis. During fibrosis, however, little is known about the contribution of HCV to fibrogenesis.

HCV is a positive-strand RNA virus with a genome that encodes an approximately 3000-amino-acid (aa) polyprotein, which is co- and post-translationally processed by proteolysis into ten mature proteins, consisting of a capsid (core), two envelope (E1, E2), and seven non-structural (NS) proteins (p7, NS2, NS3, NS4A, NS4B, NS5A, and NS5B) [1,7]. Past investigations of HCV have been limited because no suitable HCV culture systems were available to observe all steps of the viral life cycle, including entry, replication, translation, assembly, and secretion. In 1999, however, Lohmann et al. [8] developed a subgenomic replicon (SGR) system using replicon RNA encoding NS proteins (NS3-NS5B) for the analysis of RNA replication and translation [8]. In addition, an HCV pseudo-particle system (HCVpp) based on HIV and MMLV was developed for viral entry analysis [9,10].

Recently, HCV strain JFH-1, which was isolated from a Japanese patient with fulminant hepatitis, has permitted all steps of the HCV life cycle to be examined in a cultured cell line [11]. Replication of the transfected JFH-1 genome in host cells was restricted to the human hepatoma cell line Huh7 or its derivatives. Hepatocytes

* Corresponding author. Address: Department of Virology II, National Institute of Infectious Diseases, 1-23-1 Toyama, Shinjuku-ku, Tokyo 162-8640, Japan. Fax: +81 3 5285 1161.
E-mail address: wakita@nih.go.jp (T. Wakita).

0006-291X/$ - see front matter © 2011 Elsevier Inc. All rights reserved.
doi:10.1016/j.bbrc.2011.02.125

are thought to be permissive for HCV infection because liver tissue is a major target organ for HCV infection. However, virus replication levels in HCV patients are typically too low to detect the distribution of viral proteins in liver biopsies by antibodies directed against HCV proteins, and no clear evidence indicates which cell groups are the major target of HCV infection. Thus, it is unclear whether hepatic cells are the only target of HCV infection in liver tissue, and if other cells, particularly HSCs, can serve as hosts for HCV replication.

Here, we established HCV-replicating hepatic stellate cells to address whether these cells can be a potential target of HCV infection. Furthermore, we analyzed gene expression profiles of ECM-related molecules in HCV-replicating stellate cell clones to investigate the effect of HCV RNA replication on hepatic stellate cell functions.

2. Materials and methods

2.1. Cells and reagents

Human hepatic stellate cells, TWNT-4 JP7 cells derived from the LI90 cell line [12,13], were maintained in D-MEM supplemented with 10% fetal bovine serum (FBS), 100 unit/ml penicillin, 100 μg/ml streptomycin, 10 mM Hepes (pH 7.4), 1 mM sodium pyruvate, and MEM Non-Essential Amino Acids. Electroporated TWNT-4 JP7 cells and isolated SGR cells were maintained in prepared D-MEM containing either 500 or 1000 μg/ml G418. SGR Huh7 cell lines (JFH-1/4-1, JFH-1/4-5, Con1 NK5.1/0-6, and Con1 NK5.1/0-11) were maintained in prepared D-MEM containing 500 μg/ml G418 [14]. Rabbit polyclonal antibodies against NS3 and NS5A proteins were raised by immunization with recombinant NS proteins (NS3, 1195–1661 aa; NS5A, 2001–2441 aa).

2.2. Transfection and isolation of SGR clones

JFH-1 SGR RNA was synthesized using a Megascript T7 Kit with linearized pSGR-JFH-1 and pSGR-JFH-1 GND plasmids as templates. Ten micrograms HCV RNA was electroporated into 2×10^6 TWNT-4 JP7 cells, as previously described [15], which were then cultured for 3 weeks under G418 selection (500 and 1000 μg/ml). Single colonies were isolated, and the selected SGR clones were expanded and stored at −80 °C until used for analysis.

2.3. Quantification of HCV RNA in SGR cells

Total RNA was purified from each SGR clone using ISOGEN (Nippon Gene), as directed by the manufacturer's protocol. The HCV RNA copy number of each SGR clone was analyzed by a real-time PCR method, as described previously [16].

2.4. Western blot analysis

Twenty micrograms of cell lysates were separated on 10% polyacrylamide gels and then transferred to nitrocellulose membranes. Membranes were first blocked with 2% skim milk in TBS-T (20 mM Tris–HCl [pH 7.2], 500 mM NaCl, and 0.01% Tween20) and then incubated with 2% skim milk in TBS-T containing primary antibody (α-NS3 or α-NS5A), followed by secondary antibody (α-rabbit IgG HRP-conjugated). After washing membranes, bands were detected by Enhanced Chemiluminescence (ECL) Plus reagent (GE Healthcare). Luminescence signals were analyzed using the LAS-3000 Mini image analysis system (Fujifilm).

2.5. Immuno-staining of non-structural HCV proteins

Isolated SGR cells were fixed with acetone-methanol. Fixed cells were dried and incubated with primary antibodies (rabbit polyclonal α-NS3 or α-NS5A), followed by secondary antibody (α-rabbit IgG-Alexa488). Both antibodies were diluted in Block Ace (DS Pharma Biomedical) prior to use. Fluorescence of NS proteins was visualized using a Biozero microscope (Keyence).

2.6. Gene expression analysis of ECM-related genes

Total RNA was purified from SGR clones in growth phase using ISOGEN-LS (Nippon Gene). cDNA was synthesized from total RNA using random primers and Superscript III (Invitrogen). TaqMan array plates (Custom Format) were purchased from Applied Biosystems. Information of ECM-related genes in the Custom Format plate is listed in Table 1S. cDNA (55 ng/reaction) was mixed with an equal volume of TaqMan Gene Expression Master Mix (Applied Biosystems) and real-time PCR was performed using a 7500 FAST Real-Time PCR System (Applied Biosystems).

3. Results

3.1. Isolation of SGR cells

To evaluate the potential of HCV to replicate in human hepatic stellate cells and examine the role of HCV replication and viral protein in liver fibrogenesis, we established HCV SGR cells from human hepatic stellate cells. We first examined the colony formation efficiency of HCV SGR transfected into hepatic stellate cells using JFH-1 SGR RNA (Fig. 1A), which was electroporated into the human hepatic stellate cell line, TWNT-4 JP7. The transfected cells were selected using G418 for 3 weeks, and the resulting colonies were stained by crystal violet. Interestingly, many colonies (~150) were formed on transfection of cells with 10 μg JFH-1 RNA; however, no colonies were detected among cells transfected with a HCV replication-defective mutant, JFH-1 GND (Fig. 1B). This result indicated that TWNT-4 JP7 cells can support HCV replication, although colony formation efficiency of TWNT-4 JP7 cells transfected with JFH-1 SGR was much lower than that in transfected Huh7 cells (data not shown).

Next, we selected colonies of JFH-1 SGR-transfected cells and established a number of SGR TWNT-4 JP7 clones; SGR clones #1–8 and clones #11–18 were isolated from 500 and 1000 μg/ml G418 selection, respectively. The HCV RNA copy number of each SGR clone was measured by real-time RT-PCR, which revealed that the clones contained RNA copy numbers ranging from 10^4 to 10^7 copies per μg total RNA (Table 1).

Among the isolated SGR clones, we focused on SGR #1 and #2 for further analyses, because these two clones allowed HCV RNA replication at a relatively low RNA copy number compared with the other examined SGR clones. SGR #1 and #2 were cultured for an additional 8 weeks in G418 selection medium, during which time the HCV RNA copy number in both clones increased from 10^4 to 10^7 copies, which represented increases of 3200- and 470-fold, respectively (Table 2). This observed increase suggested that the occurrence of viral adaptive mutations or modifications of cellular factors during cell passaging resulted in the increased efficiency of viral RNA replication in hepatic stellate cells. We thus determined the viral RNA sequences in clones SGR #1 and #2 and some other additional clones, and identified several synonymous and non-synonymous mutations in the HCV RNA sequences (data not shown). Although two common non-synonymous mutations were found in the NS4B and NS5A gene-encoding regions, these mutations did not increase HCV RNA replication in human

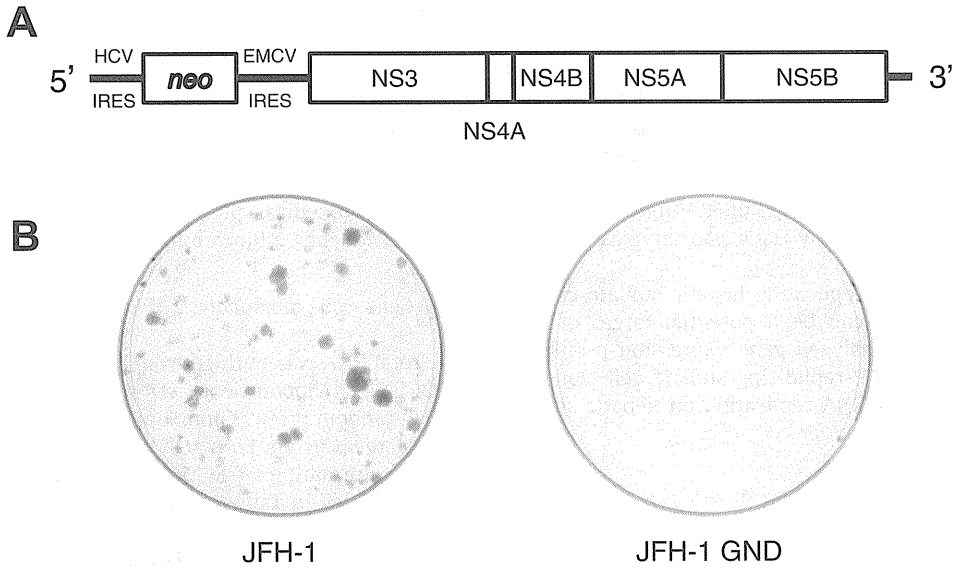

Fig. 1. Structure of the JFH-1 subgenomic replicon (SGR) and colony formation of SGR TWNT-4 JP7 cells. (A) Diagram of the JFH-1 SGR. (B) Colony formation of SGR TWNT-4 JP7 cells. TWNT-4 JP7 cells were transfected with either wild-type JFH-1 or replication-defective GND SGR RNA, and transfected cells were then cultured in G418 selection medium for 3 weeks. Cells were then fixed using formalin, and colonies were visualized by crystal violet staining. (For interpretation of the references to color in this figure legend, the reader is referred to the web version of this article.)

Table 1
RNA copy number of isolated subgenomic replicon (SGR) clones.

SGR clone	HCV RNA copy number (copies/μg of total RNA)
#1	1.5×10^4
#2	5.3×10^4
#3	9.4×10^5
#4	2.3×10^5
#5	1.7×10^5
#6	1.5×10^4
#7	4.2×10^5
#8	1.3×10^6
Average	3.9×10^5
#11	3.8×10^5
#12	1.2×10^7
#13	4.8×10^5
#14	2.3×10^6
#15	4.7×10^5
#16	2.1×10^6
#17	5.1×10^5
#18	2.0×10^6
Average	2.5×10^6

Table 2
Change of RNA copy number in isolated subgenomic replicon (SGR) clones following long-term culture.

SGR clone	4 weeks*	12 weeks*
#1	1.5×10^4	4.9×10^7
#2	5.3×10^4	2.5×10^7

* Copies/μg of total RNA.

hepatic stellate cells when they were artificially introduced into the replicon genome (data not shown).

3.2. Expression of non-structural HCV proteins

The expression of several NS HCV proteins, from NS3 to NS5B, is required for HCV RNA replication in infected cells. It is reported that these NS proteins form complexes to replicate HCV RNA, with NS5A protein in particular localizing to specialized membranous web structures around lipid droplets, which are considered to serve as the scaffold for HCV RNA replication and assembly [17,18]. To confirm the expression of NS proteins in isolated SGR clones, we performed western blotting and immunostaining of HCV NS proteins (Fig. 2). As shown in Fig. 2A, NS3 and NS5A proteins of expected size were detected by western blotting in SGR #1 and #2 cells. The expression of both NS3 and NS5A in SGR #1 was higher than that in SGR #2, a result that is consistent with the determined viral RNA copy number of each clone (Table 2). Immunostaining of NS proteins clearly showed cytoplasmic distribution, similar to that observed in Huh7 cells (Fig. 2B). Specifically, the fluorescence of NS5A was distributed as a fine reticular pattern with occasional granular staining. These results demonstrated that HCV RNA replicated in hepatic stellate cells and that HCV NS proteins were expressed in hepatic stellate cells at identical levels as in Huh7 cells.

3.3. Gene expression profiles of ECM-related molecules in SGR cells

In liver tissue, once stellate cells are activated by inflammation mediators secreted from infected or injured cells, the activated cells differentiate into myoblast cells. In addition, ECM-related molecule gene expression is altered, which leads to the progression of liver fibrosis. Here, we examined if HCV RNA replication in stellate cells affects the gene expression of ECM-related molecules by measuring gene expression in both parental TWNT-4 JP7 and isolated SGR cells using a TaqMan array plate (Custom Format) consisting of 24 selected genes from the collagen (COL), MMP, and TIMP families (Table 1S) [19,20]. Among the 16 isolated SGR clones in this study, 10 in growth phase were examined for ECM-related molecule gene expression. All SGR clones exhibited a decrease of collagen gene expression compared with parental TWNT-4 JP7 cells. In particular, four collagen genes (COL1A1, COL4A2, COL5A1, and COL15A1) were expressed at levels approximately 0.5-fold lower than those of parental cells (Fig. 3A), whereas MMP1, MMP3, and MMP12 increased 4-, 5.6-, and 4.8-fold, respectively (Fig. 3B). These results suggest that HCV RNA replication or viral proteins in hepatic stellate cells down- and up-regulate COL and MMP gene expression, respectively.

To determine if gene expression changes of ECM-related molecules in isolated SGR clones were specific to hepatic stellate cells,

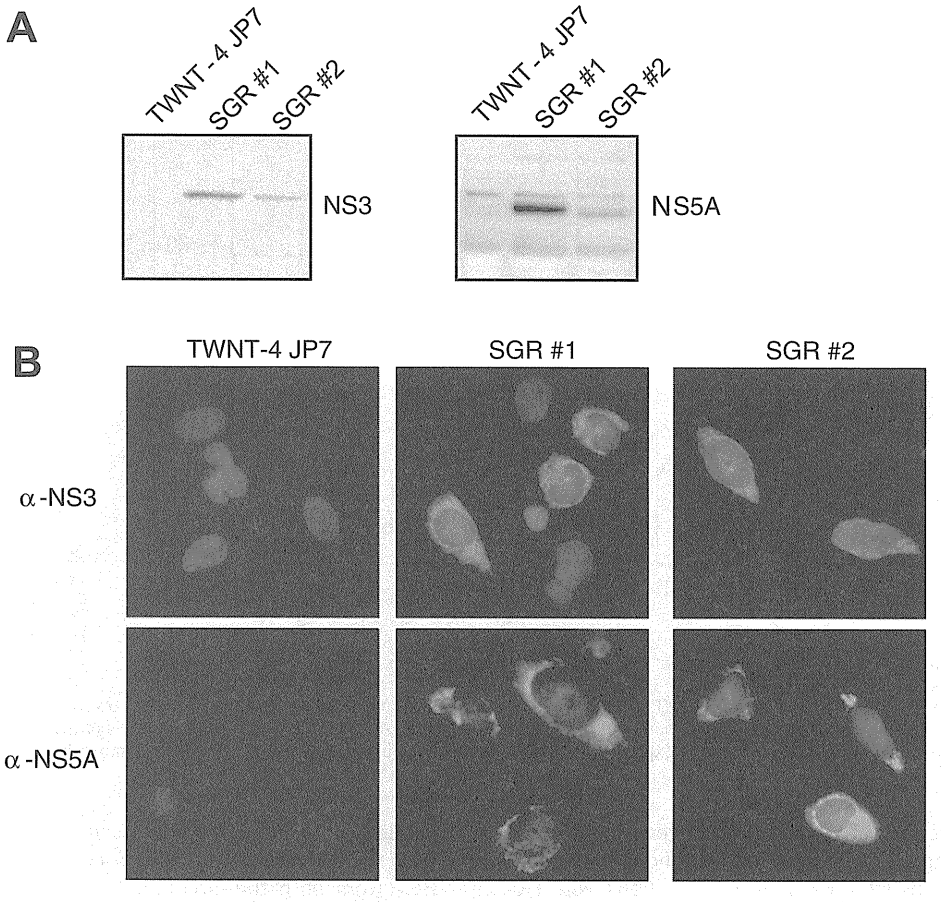

Fig. 2. Expression of non-structural (NS) NS3 and NS5A proteins in isolated SGR clones. (A) Total cell lysates of TWNT-4 JP7 and SGR clones were separated by SDS–PAGE and transferred to a nitrocellulose membrane. HCV NS proteins NS3 and NS5A were detected by western blot analysis with rabbit polyclonal α-NS3 and α-NS5A antibodies. (B) The expression of HCV NS proteins were also observed by immuno-staining with rabbit polyclonal α-NS3 and α-NS5A antibodies (blue, nuclear; green, NS proteins). (For interpretation of the references to color in this figure legend, the reader is referred to the web version of this article.)

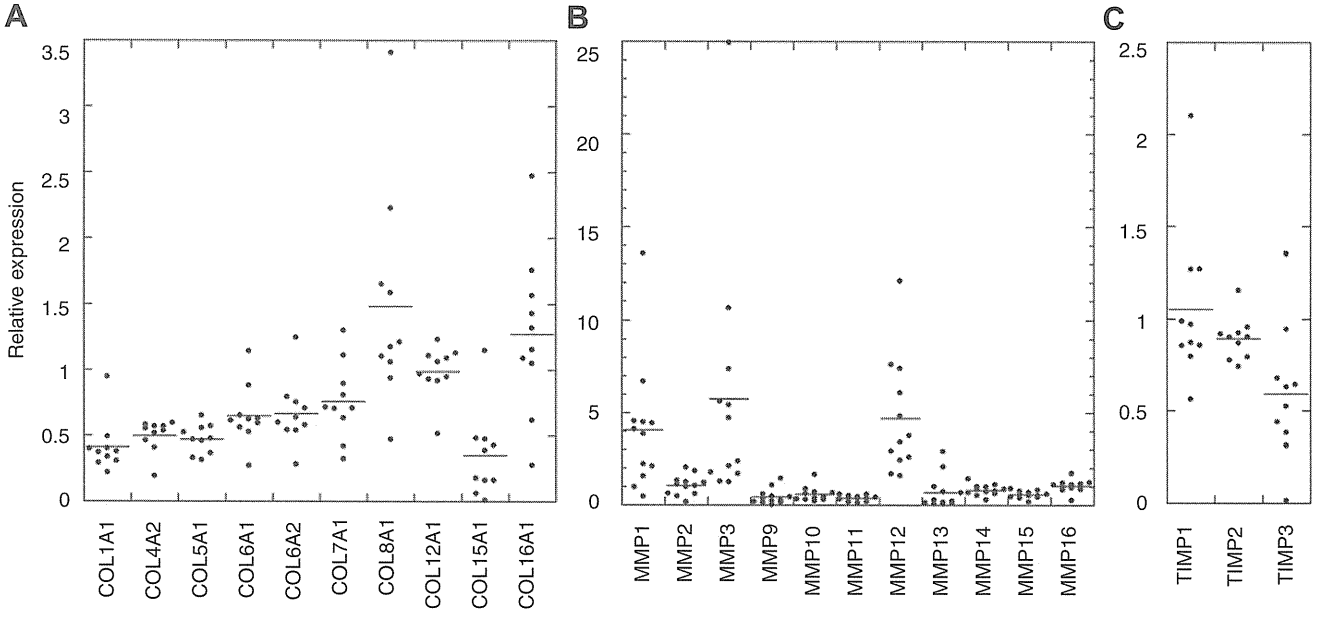

Fig. 3. Relative expression levels of extracellular matrix (ECM)-related genes in isolated TWNT-4 SGR clones. Gene expression levels of collagen (A), matrix metalloproteinase (B), and tissue inhibitor of metalloproteinase genes (C) were measured by TaqMan PCR. The expression levels of the indicated ECM-related genes were normalized to those of parental TWNT-4 JP7 cells. Values of gene expression level are summarized in Supplementary Table 2S. The bar in each column indicates the average.

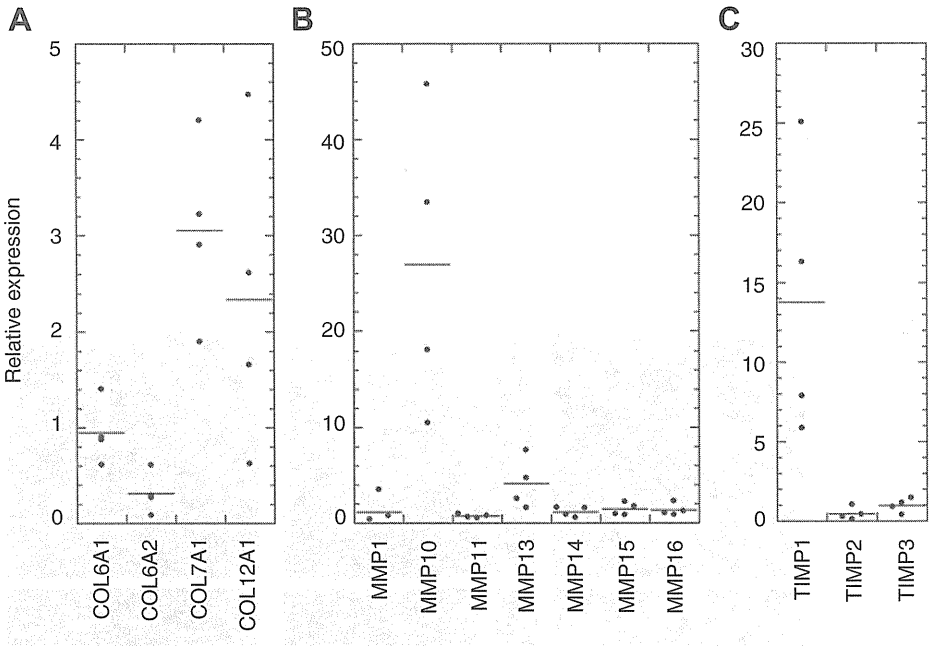

Fig. 4. Relative expression levels of extracellular matrix (ECM)-related genes in subgenomic replicon Huh7 clones. Gene expression levels of collagen (A), matrix metalloproteinase (B), and tissue inhibitor of metalloproteinase genes (C) were measured by TaqMan PCR. The expression levels of the indicated ECM-related genes were normalized to those of parental Huh7 cells. Values of gene expression levels are summarized in Table 3S. The bar in each column indicates the average.

we analyzed the expression of the identical 24 genes in SGR hepatic cells. The gene expression levels of four SGR hepatic cell clones derived from Huh7 cells (JFH-1/4-1, JFH-1/4-5, Con1 NK5.1/0-6, and Con1 NK5.1/0-11) were also measured by TaqMan array analysis (Fig. 4). Distinct differences in gene expression profiles were observed between hepatic and hepatic stellate cells, and the expression of several genes were not detected in Huh7 cells. In SGR Huh7 cells, COL7A1 and COL12A1 gene expression increased greater than 2-fold (Fig. 4A), while the expression of the COL1A1 gene increased from undetectable to detectable levels (data not shown). In addition, MMP10, MMP13, and TIMP1 gene expression was markedly increased in hepatic replicon cells compared with the levels in Huh7 cells (Fig. 4B and C).

4. Discussion

In previous studies, a few SGR cell lines were established from different HCV strains (JFH-1, H77, and Con-1) and several human cell lines (Huh7, HepG2, IMY-N9, HeLa, and 293 cells) [8,21,22]. The combination of JFH-1 SGR and Huh7 cells exhibited increased RNA replication without adaptive mutations compared with H77 and Con-1 strains. Furthermore, full genomic JFH-1 and its chimera virus have been shown to infect Huh7 and derivatives. Although we did not observe HCV infection using the combination of JFH-1 and the TWNT-4 JP7 cell line (data not shown), this is the first study to isolate SGR clones using hepatic stellate cells. Our findings indicate that hepatic stellate cells potentially support HCV replication in infected livers.

A total of 16 SGR clones were isolated from SGR RNA-transfected TWNT-4 JP7 cells in this study. The HCV RNA copy number in the selected clones clearly differed between the two concentrations of G418 used for selection, with 500 and 1000 μg/ml G418 yielding an average RNA copy numbers of 3.9×10^5 and 2.5×10^6, respectively (Table 1). Although RNA replication in SGR clones was lower than that observed in hepatic replicon cells, such as Huh7 and IMY-N9 cells, the RNA copy number of SGR clones selected using 1000 μg/ml G418 was comparable to that of non-hepatic replicon cells derived from HeLa and 293 cell lines [21,22]. Since hepatic stellate cells localize in liver tissue where HCV replicates, hepatic stellate cells are likely to be exposed to HCV from both the circulation system and neighboring hepatocytes. Cell-to-cell HCV transmission was also reported in recent studies [23,24], further supporting our results that hepatic stellate cells are a possible target of HCV infection.

It was reported that a number of adaptive mutations in the HCV genomic sequence increase viral production in infected cells and RNA replication in SGR cells [25–27]. Here, isolated replicon cells exhibited increased RNA replication during an additional 8 weeks of culture, and several mutations were identified in the sequenced HCV RNA of SGR cells. Clones SGR #1 and #2 contained four synonymous and three non-synonymous mutations, respectively. Although we performed a colony forming assay by transfection of SGR RNA containing these mutations into TWNT-4 JP7 cells, no differences in colony formation were observed between wild-type and mutant RNA-transfected cells (data not shown). This finding suggests that modification of certain cellular factors may have occurred in the SGR clones during cell passage, rather than the appearance of adaptive mutations in the replicon genome.

From the results of our TaqMan analysis, the expression of several collagen genes were significantly down-regulated and three MMP genes (MMP1, MMP3, and MMP12) were up-regulated in isolated SGR clones compared with parental TWNT-4 JP7 cells (Fig. 3). Type I and IV collagen are important for liver fibrogenesis, and MMP-1 degrades type I collagen to regulate ECM regeneration in liver tissue [19]. Furthermore, MMP-3 regulates MMP-1 activation [28,29], while overproduction of MMP-12 causes ECM protein breakdown and excessive remodeling, which has been implicated in a range of respiratory diseases [30–32]. Although no relationship between HCV RNA copy number and the expression of these genes in SGR cells was detected, a certain degree of HCV RNA replication may be sufficient to influence the regulation of ECM-related genes. Taken together, these findings suggest that HCV RNA-replicating hepatic stellate cells may suppress ECM production and negatively regulate hepatic fibrosis. In contrast, increased expression of type I collagen and TIMP-1 genes, an inhibitor of MMP-1, was observed in hepatic replicon cells, suggesting that hepatic cells up-regulate

ECM accumulation through collagen production and the inhibition of MMP activity. As hepatic cells are the major cell group in liver tissue, HCV-infected hepatic cells may be one of the factors promoting fibrosis by producing ECM proteins such as type I collagen and TIMP-1. Our results indicate that although HCV RNA replication and/or HCV NS proteins affect gene expression of EMC-related molecules in both hepatic stellate cells and hepatic cells, the gene expression profiles differ between these cell types. Further studies are necessary to analyze the mechanisms of ECM-related gene expression in HCV-infected livers.

Primary hepatic stellate cells isolated from liver tissue typically transform into myofibroblastic cells (active formation) during subsequent passages. As the TWNT-4 JP7 cells used in this study also exhibited an activated phenotype [13,33], the results of our gene expression analyses may reflect the phenotype of activated hepatic stellate cells. In fact, it is presently difficult to isolate and maintain quiescent hepatic stellate cell populations. Although *in vitro* culture systems involving primary cells and hepatic stellate cell lines are valuable tools for studying liver fibrosis, SGR cells generated from quiescent hepatic stellate cells are required for the detailed analysis of hepatic stellate cell functions in fibrosis.

In conclusion, our study has shown that HCV RNA replicates in human hepatic stellate cells and affects the gene expression of ECM-related molecules, suggesting the potential of HCV to infect and directly influence ECM-related gene regulation in hepatic stellate cells. The HCV RNA-replicating hepatic stellate cell line isolated in this study is useful not only for investigating hepatic stellate cell functions, but also for studying HCV replication machinery.

Acknowledgments

This work was partially supported by a grant-in-aid for Scientific Research from the Japan Society for the Promotion of Science, the Ministry of Health Labor and Welfare of Japan, the Japan Health Sciences Foundation, and the National Institute of Biomedical Innovation.

Appendix A. Supplementary data

Supplementary data associated with this article can be found, in the online version, at doi:10.1016/j.bbrc.2011.02.125.

References

[1] J.M. Pawlotsky, Pathophysiology of hepatitis C virus infection and related liver disease, Trends Microbiol. 12 (2004) 96–102.
[2] F.V. Chisari, Unscrambling hepatitis C virus-host interactions, Nature 436 (2005) 930–932.
[3] J.J. Feld, J.H. Hoofnagle, Mechanism of action of interferon and ribavirin in treatment of hepatitis C, Nature 436 (2005) 967–972.
[4] S.L. Friedman, M.B. Bansal, Reversal of hepatic fibrosis–fact or fantasy?, Hepatology 43 (2006) S82–88
[5] J.P. Iredale, Models of liver fibrosis: exploring the dynamic nature of inflammation and repair in a solid organ, J. Clin. Invest. 117 (2007) 539–548.
[6] S.L. Friedman, Hepatic stellate cells: protean, multifunctional, and enigmatic cells of the liver, Physiol. Rev. 88 (2008) 125–172.
[7] R. Bartenschlager, Hepatitis C virus molecular clones: from cDNA to infectious virus particles in cell culture, Curr. Opin. Microbiol. 9 (2006) 416–422.
[8] V. Lohmann, F. Korner, J. Koch, U. Herian, L. Theilmann, R. Bartenschlager, Replication of subgenomic hepatitis C virus RNAs in a hepatoma cell line, Science 285 (1999) 110–113.
[9] B. Bartosch, J. Dubuisson, F.L. Cosset, Infectious hepatitis C virus pseudo-particles containing functional E1–E2 envelope protein complexes, J. Exp. Med. 197 (2003) 633–642.
[10] M. Hsu, J. Zhang, M. Flint, C. Logvinoff, C. Cheng-Mayer, C.M. Rice, J.A. McKeating, Hepatitis C virus glycoproteins mediate pH-dependent cell entry of pseudo typed retroviral particles, Proc. Natl. Acad. Sci. USA 100 (2003) 7271–7276.
[11] T. Wakita, T. Pietschmann, T. Kato, T. Date, M. Miyamoto, Z. Zhao, K. Murthy, A. Habermann, H.G. Krausslich, M. Mizokami, R. Bartenschlager, T.J. Liang, Production of infectious hepatitis C virus in tissue culture from a cloned viral genome, Nat. Med. 11 (2005) 791–796.
[12] K. Murakami, T. Abe, M. Miyazawa, M. Yamaguchi, T. Masuda, T. Matsuura, S. Nagamori, K. Takeuchi, K. Abe, M. Kyogoku, Establishment of a new human cell line, LI90, exhibiting characteristics of hepatic Ito (fat-storing) cells, Lab. Invest. 72 (1995) 731–739.
[13] N. Shibata, T. Watanabe, T. Okitsu, M. Sakaguchi, M. Takesue, T. Kunieda, K. Omoto, S. Yamamoto, N. Tanaka, N. Kobayashi, Establishment of an immortalized human hepatic stellate cell line to develop antifibrotic therapies, Cell Transplant. 12 (2003) 499–507.
[14] M. Miyamoto, T. Kato, T. Date, M. Mizokami, T. Wakita, Comparison between subgenomic replicons of hepatitis C virus genotypes 2a (JFH-1) and 1b (Con1 NK5.1), Intervirology 49 (2006) 37–43.
[15] T. Kato, T. Date, A. Murayama, K. Morikawa, D. Akazawa, T. Wakita, Cell culture and infection system for hepatitis C virus, Nat. Protoc. 1 (2006) 2334–2339.
[16] T. Takeuchi, A. Katsume, T. Tanaka, A. Abe, K. Inoue, K. Tsukiyama-Kohara, R. Kawaguchi, S. Tanaka, M. Kohara, Real-time detection system for quantification of hepatitis C virus genome, Gastroenterology 116 (1999) 636–642.
[17] B. Wolk, B. Buchele, D. Moradpour, C.M. Rice, A dynamic view of hepatitis C virus replication complexes, J. Virol. 82 (2008) 10519–10531.
[18] Y. Miyanari, K. Atsuzawa, N. Usuda, K. Watashi, T. Hishiki, M. Zayas, R. Bartenschlager, T. Wakita, M. Hijikata, K. Shimotohno, The lipid droplet is an important organelle for hepatitis C virus production, Nat. Cell Biol. 9 (2007) 1089–1097.
[19] M.J. Arthur, Fibrogenesis II, Metalloproteinases and their inhibitors in liver fibrosis, Am. J. Physiol. Gastrointest. Liver Physiol. 279 (2000) G245–G249.
[20] H.J. Ra, W.C. Parks, Control of matrix metalloproteinase catalytic activity, Matrix Biol. 26 (2007) 587–596.
[21] T. Date, T. Kato, M. Miyamoto, Z. Zhao, K. Yasui, M. Mizokami, T. Wakita, Genotype 2a hepatitis C virus subgenomic replicon can replicate in HepG2 and IMY-N9 cells, J. Biol. Chem. 279 (2004) 22371–22376.
[22] T. Kato, T. Date, M. Miyamoto, Z. Zhao, M. Mizokami, T. Wakita, Nonhepatic cell lines HeLa and 293 support efficient replication of the hepatitis C virus genotype 2a subgenomic replicon, J. Virol. 79 (2005) 592–596.
[23] J.M. Timpe, Z. Stamataki, A. Jennings, K. Hu, M.J. Farquhar, H.J. Harris, A. Schwarz, I. Desombere, G.L. Roels, P. Balfe, J.A. McKeating, Hepatitis C virus cell-cell transmission in hepatoma cells in the presence of neutralizing antibodies, Hepatology 47 (2008) 17–24.
[24] J. Witteveldt, M.J. Evans, J. Bitzegeio, G. Koutsoudakis, A.M. Owsianka, A.G. Angus, Z.Y. Keck, S.K. Foung, T. Pietschmann, C.M. Rice, A.H. Patel, CD81 is dispensable for hepatitis C virus cell-to-cell transmission in hepatoma cells, J. Gen. Virol. 90 (2009) 48–58.
[25] R.S. Russell, J.C. Meunier, S. Takikawa, K. Faulk, R.E. Engle, J. Bukh, R.H. Purcell, S.U. Emerson, Advantages of a single-cycle production assay to study cell culture-adaptive mutations of hepatitis C virus, Proc. Natl. Acad. Sci. USA 105 (2008) 4370–4375.
[26] D. Delgrange, A. Pillez, S. Castelain, L. Cocquerel, Y. Rouille, J. Dubuisson, T. Wakita, G. Duverlie, C. Wychowski, Robust production of infectious viral particles in Huh-7 cells by introducing mutations in hepatitis C virus structural proteins, J. Gen. Virol. 88 (2007) 2495–2503.
[27] J. Zhong, P. Gastaminza, J. Chung, Z. Stamataki, M. Isogawa, G. Cheng, J.A. McKeating, F.V. Chisari, Persistent hepatitis C virus infection in vitro: coevolution of virus and host, J. Virol. 80 (2006) 11082–11093.
[28] K. Suzuki, H. Nagase, A. Ito, J.J. Enghild, G. Salvesen, The role of matrix metalloproteinase 3 in the stepwise activation of human rheumatoid synovial procollagenase, Biol. Chem. Hoppe Seyler 371 (Suppl.) (1990) 305–310.
[29] G. Murphy, M.I. Cockett, P.E. Stephens, B.J. Smith, A.J. Docherty, Stromelysin is an activator of procollagenase. A study with natural and recombinant enzymes, Biochem. J. 248 (1987) 265–268.
[30] S. Nenan, E. Boichot, V. Lagente, C.P. Bertrand, Macrophage elastase (MMP-12): a pro-inflammatory mediator?, Mem Inst. Oswaldo Cruz 100 (Suppl. 1) (2005) 167–172.
[31] T.J. Gronski Jr., R.L. Martin, D.K. Kobayashi, B.C. Walsh, M.C. Holman, M. Huber, H.E. Van Wart, S.D. Shapiro, Hydrolysis of a broad spectrum of extracellular matrix proteins by human macrophage elastase, J. Biol. Chem. 272 (1997) 12189–12194.
[32] S. Chandler, J. Cossins, J. Lury, G. Wells, Macrophage metalloelastase degrades matrix and myelin proteins and processes a tumour necrosis factor-alpha fusion protein, Biochem. Biophys. Res. Commun. 228 (1996) 421–429.
[33] N. Higashi, M. Kohjima, M. Fukushima, S. Ohta, K. Kotoh, M. Enjoji, N. Kobayashi, M. Nakamuta, Epigallocatechin-3-gallate, a green-tea polyphenol, suppresses Rho signaling in TWNT-4 human hepatic stellate cells, J. Lab. Clin. Med. 145 (2005) 316–322.

Virology 410 (2011) 38–47

Contents lists available at ScienceDirect

Virology

journal homepage: www.elsevier.com/locate/yviro

Chaperonin TRiC/CCT participates in replication of hepatitis C virus genome via interaction with the viral NS5B protein

Yasushi Inoue [a,b,c], Hideki Aizaki [a], Hiromichi Hara [a], Mami Matsuda [a], Tomomi Ando [a], Tetsu Shimoji [a], Kyoko Murakami [a], Takahiro Masaki [a], Ikuo Shoji [d], Sakae Homma [b], Yoshiharu Matsuura [e], Tatsuo Miyamura [a], Takaji Wakita [a], Tetsuro Suzuki [a,f,*]

[a] Department of Virology II, National Institute of Infectious Diseases, Tokyo 162-8640, Japan
[b] Department of Respiratory Medicine, Toho University School of Medicine, Tokyo 143-8541, Japan
[c] International University of Health and Welfare, Mita Hospital, Tokyo 108-8329, Japan
[d] Division of Microbiology, Kobe University Graduate School of Medicine, Hyogo 650-0017, Japan
[e] Research Institute for Microbial Diseases, Osaka University, Osaka 565-0871, Japan
[f] Department of Infectious Diseases, Hamamatsu University School of Medicine, Hamamatsu 431-3192, Japan

ARTICLE INFO

Article history:
Received 12 June 2010
Returned to author for revision 18 July 2010
Accepted 15 October 2010
Available online 18 November 2010

Keywords:
Hepatitis C virus
Replication
Non-structural protein
Chaperonin

ABSTRACT

To identify the host factors implicated in the regulation of hepatitis C virus (HCV) genome replication, we performed comparative proteome analyses of HCV replication complex (RC)-rich membrane fractions prepared from cells harboring genome-length bicistronic HCV RNA at the exponential and stationary growth phases. We found that the eukaryotic chaperonin T-complex polypeptide 1 (TCP1)-ring complex/chaperonin-containing TCP1 (TRiC/CCT) plays a role in the replication possibly through an interaction between subunit CCT5 and the viral RNA polymerase NS5B. siRNA-mediated knockdown of CCT5 suppressed RNA replication and production of the infectious virus. Gain-of-function activity was shown following co-transfection with whole eight TRiC/CCT subunits. HCV RNA synthesis was inhibited by an anti-CCT5 antibody in a cell-free assay. These suggest that recruitment of the chaperonin by the viral nonstructural proteins to the RC, which potentially facilitate folding of the RC component(s) into the mature active form, may be important for efficient replication of the HCV genome.

Introduction

Hepatitis C virus (HCV) is a major cause of chronic liver diseases, such as chronic hepatitis, hepatic steatosis, cirrhosis, and hepatocellular carcinoma (Hoofnagle, 2002; Manns et al., 2006; Saito et al., 1990; Seeff and Hoofnagle, 2003). HCV is an enveloped positive-strand RNA virus belonging to the *Hepacivirus* genus of the Flaviviridae family. Its genome of ~9.6 kb encodes a polyprotein precursor of ~3000 amino acids (aa) (Suzuki et al., 2007; Taguwa et al., 2008). The precursor polyprotein is post- or cotranslationally processed by both viral and host proteases into at least ten viral products. The nonstructural (NS) proteins NS3–NS5B are necessary and sufficient for autonomous HCV RNA replication. They form a membrane-associated replication complex (RC), in which NS5B is the RNA-dependent RNA polymerase (RdRp) that is responsible for copying the RNA genome of the virus during replication. The HCV RC has been detected in detergent-resistant membrane (DRM) structures, possibly in a lipid-raft structure (Aizaki et al., 2004; Shi et al., 2003). Cell-free RC replication activity has also been demonstrated in crude membrane fractions of HCV subgenomic replicon cells (Aizaki et al., 2004; Ali et al., 2002; Hara et al., 2009; Hardy et al., 2003; Yang et al., 2004); these cell-free systems provide semi-intact RdRp assays for biochemical dissection of viral replication.

In general, any process that occurs during viral replication is dependent on the host cell machinery and requires close interaction between viral and cellular proteins. Although evidence that host cell factors interact with HCV NS proteins and are involved in viral replication is accumulating (Moriishi and Matsuura, 2007), the cellular components of HCV RC and their functional roles in viral replication are not fully understood.

Recently, using comparative proteome analysis, we identified 27 cellular proteins that were highly enriched in the DRM fraction of HCV replicon cells relative to parental cells. Subsequent analyses demonstrated that one of the identified proteins, creatine kinase B, a key ATP-generating enzyme, is important for efficient replication of the HCV genome and for production of the infectious virus (Hara et al., 2009).

In this study, to extend our investigation and to increase our understanding of the precise components of HCV RC and the

* Corresponding author. Department of Infectious Diseases, Hamamatsu University School of Medicine, Hamamatsu 431-3192, Japan. Fax: +81 53 435 2337.
E-mail address: tesuzuki@hama-med.ac.jp (T. Suzuki).

0042-6822/$ – see front matter © 2010 Elsevier Inc. All rights reserved.
doi:10.1016/j.virol.2010.10.026